Electronic Supplementary Material (ESI) for Organic & Biomolecular Chemistry

The immobilisation of chiral organocatalysts on magnetic nanoparticles: the support particle cannot always be considered inert

Oliver Gleeson,[a] Gemma-Louise Davies,[b] Aldo Peschiulli,[a] Renata Tekoriute,[b] Yurii K. Gun'ko*[b] and Stephen J. Connon*[a]

[a]Centre for Synthesis and Chemical Biology, School of Chemistry, Trinity College Dublin, Dublin 2, Ireland.

[b]School of Chemistry and CRANN, Trinity College Dublin, Dublin 2, Ireland.

Contents

1.0 Characterisation of **8**

1.1 FTIR analysis

The FTIR spectra for the magnetite nanoparticles before and after loading with the bifunctional urea catalyst are shown in Figure 1. The spectrum for magnetite nanoparticles alone (black line) shows a stretching vibration at 3440 cm^{-1} which incorporates the contributions from both symmetrical (v_1) and asymmetrical (v_3) modes of the O-H bonds which are attached to the surface iron atoms. The presence of an adsorbed water layer is confirmed by a stretch for the vibrational mode of water found at 1635 cm^{-1}. In the spectra for the catalyst-loaded nanoparticles, additional stretches between 1740 and 860 cm^{-1} representing the various functionalities of the urea catalyst are noted. There appear to be very few differences between the spectra of the catalyst treated nanoparticles before and after recycling, indicating no changes or degradation of the catalyst treated magnetite nanoparticles after recycling several times.

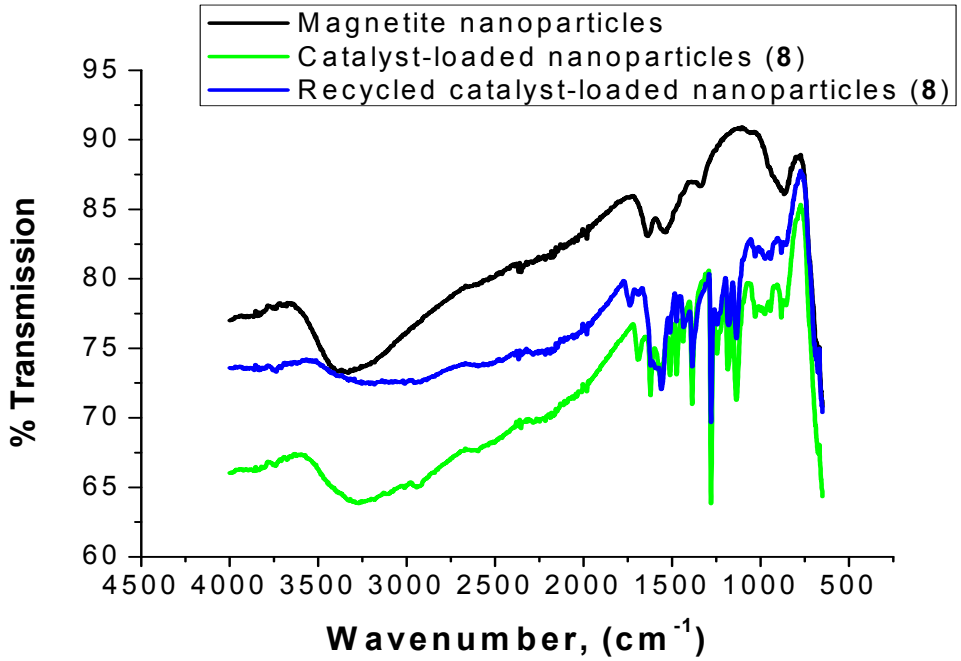

Figure 1. FTIR spectra of magnetite before loading with catalyst (black) and after loading with urea catalyst, **8** (green) and after recycling several times (blue).

1.2 TGA studies

TGA was carried out on the magnetite nanoparticles before and after treatment with the bifunctional urea catalyst (Figure 2). TGA can show bond formation between the magnetite nanoparticles and the catalyst. The total weight loss from the magnetite nanoparticles alone is ~2%. Much of this small weight percentage loss is due to the loss of strongly adsorbed water and surface hydroxyl groups from the particles which takes place between 30 and 250 ^{o}C. Slight changes in the curve after 500 ^{o}C are due to a phase change of the material from magnetite to maghemite. The curve representing compound **8**, the catalyst-loaded magnetite nanoparticles before recycling shows a total weight loss of 9.5%. The curve representing the catalyst-loaded magnetite nanoparticles after recycling shows a total weight loss of 10.8%. Above 120 ^{o}C, organic groups representative of the functionalised catalyst are desorbed from the nanoparticles. This confirms the

functionalisation of the nanoparticles with the catalyst, as expected. The difference in mass lost between the two catalyst-loaded magnetite nanoparticle samples shows that there is a slight change in the surface functionality of the nanoparticles after they are recycled. The increased mass lost from the recycled sample suggests the presence of a higher mass percentage of the organic functionality, perhaps implying a hydrolysis or adsorption process of the surface functionalities occurring over the course of multiple recycling. Examination of the D-TGA curves for the two samples (inset, Figure 2) indicates a slight shift in the temperature at which the final organic species is lost, again perhaps indicating a partial degradation of this group due to recycling.

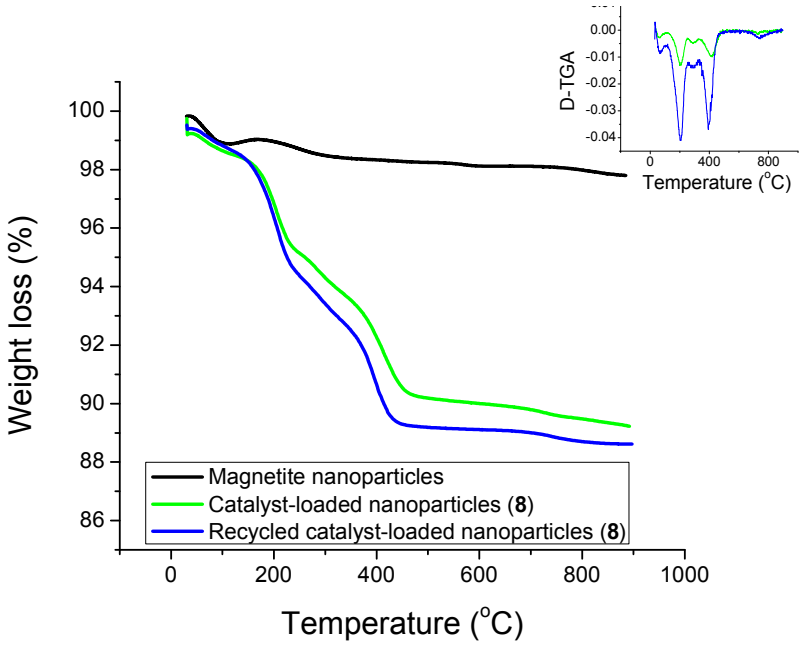

Figure 2. TGA curves of percentage mass lost on heating from 30-900°C of magnetite nanoparticles (black), urea catalyst-loaded magnetite nanoparticles (**8**) before recycling (green) and after recycling several times (blue).

1.3 XRD studies

A dry solid powder sample was used to collect XRD patterns of the sample of magnetite nanoparticles and the bifunctional urea catalyst-loaded nanoparticles before and after recycling (**Figure 3**). The observed patterns both correspond well to the JCPDS database for magnetite. The average particle size has been calculated from the peak width at half maximum of the peak at 35.5 degrees 2θ, using the Debye-Scherrer equation.[1] The average particle size was found to be 10.99 nm, which is in close agreement with the particle size as calculated from TEM. The calculated size was the same for the magnetite before and after loading with catalyst and subsequent recycling. The interlayer spacings (d_{hkl}), calculated using the Bragg equation, agree well with the data for standard magnetite (**Table 1**). The lattice parameter *a* has been calculated from the interplanar spacing of the most intense peak, which for magnetite is the (311) *hkl* line. The *a* lattice parameter was calculated as 0.840 nm, which coincides closely with the value for magnetite (0.839 nm). The peaks at 12.2 and 74 degrees 2θ appear due to the lamp present in the XRD machine. The peak at 23 degrees 2θ is due to the silica gel used to adhere the sample to the glass holder.

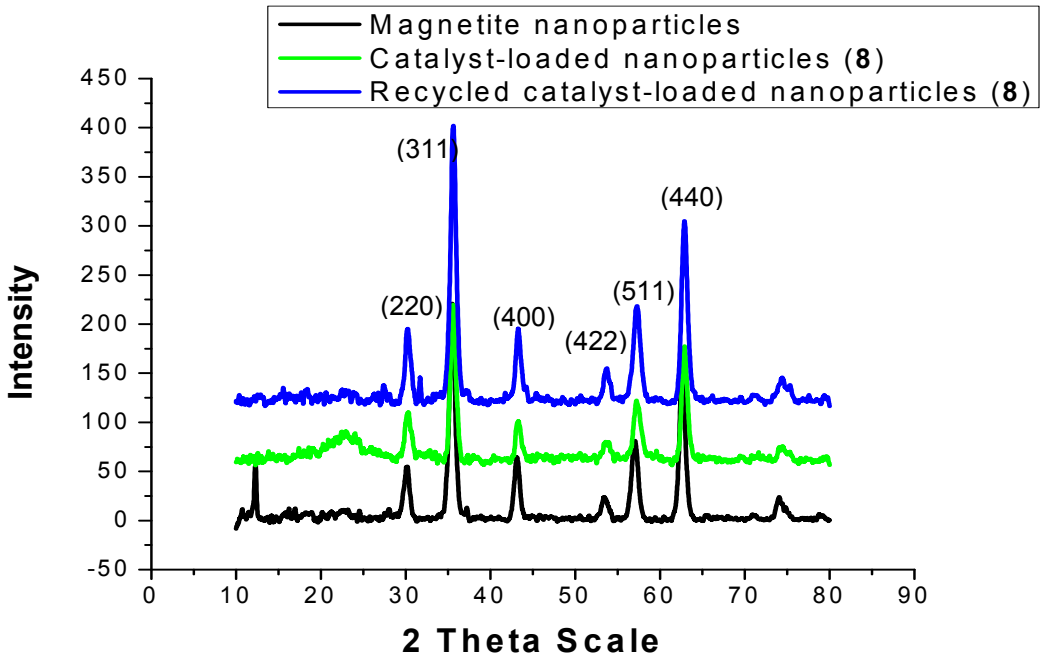

Figure 3. XRD patterns of magnetite nanoparticles (black), urea catalyst-loaded nanoparticles (8) before recycling (green) and after recycling several times (blue).

Table 1. Lattice parameters and interlayer spacings for magnetite nanoparticles

Sample	(hkl)					
	1	2	3	4	5	6
Prepared Fe_3O_4	0.296	0.253	0.210	0.171	0.161	0.148
Standard Fe_3O_4 [1]	0.296	0.253	0.209	0.171	0.161	0.148

2.0 Determination of loading of siloxane **11** by ^{1}H NMR spectroscopy

T = 0, (400MHz, $C_6D_5CD_3$)

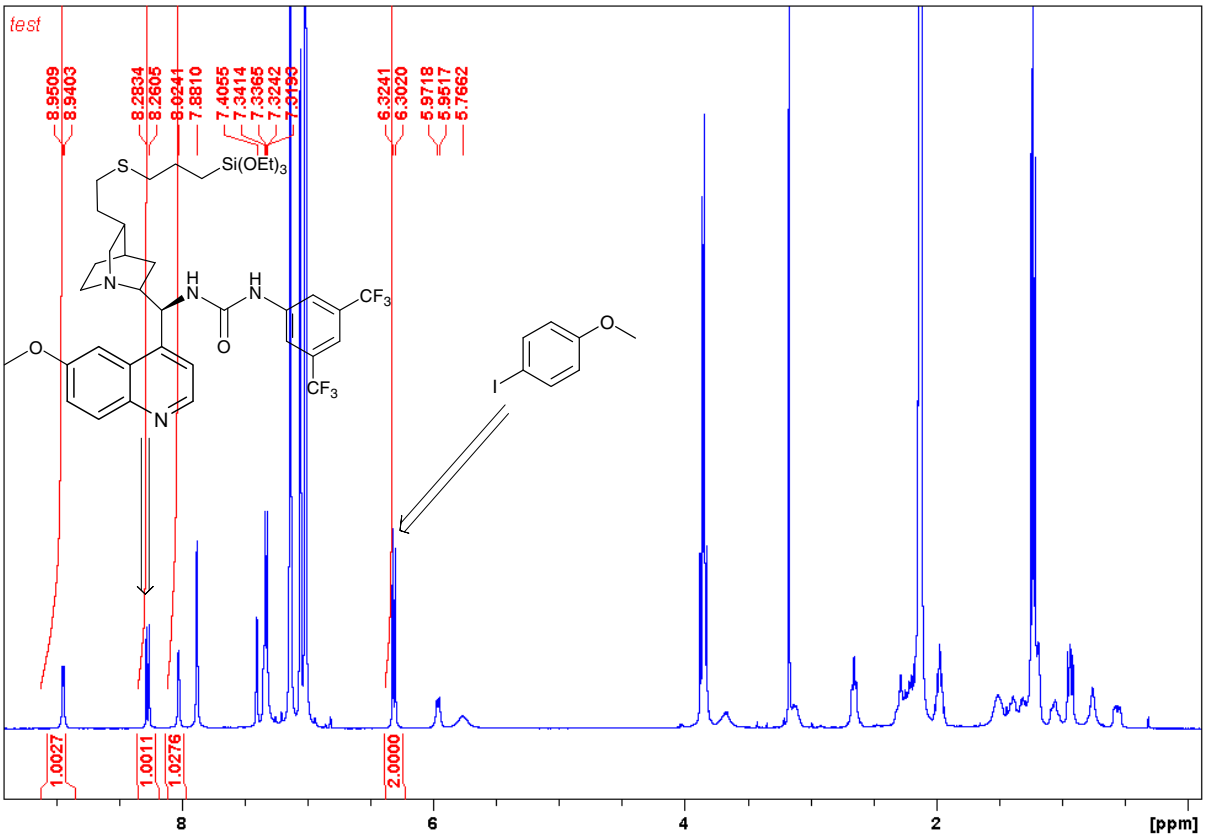

100% loading of siloxane **11** at T = 24h, (400MHz, $C_6D_5CD_3$)

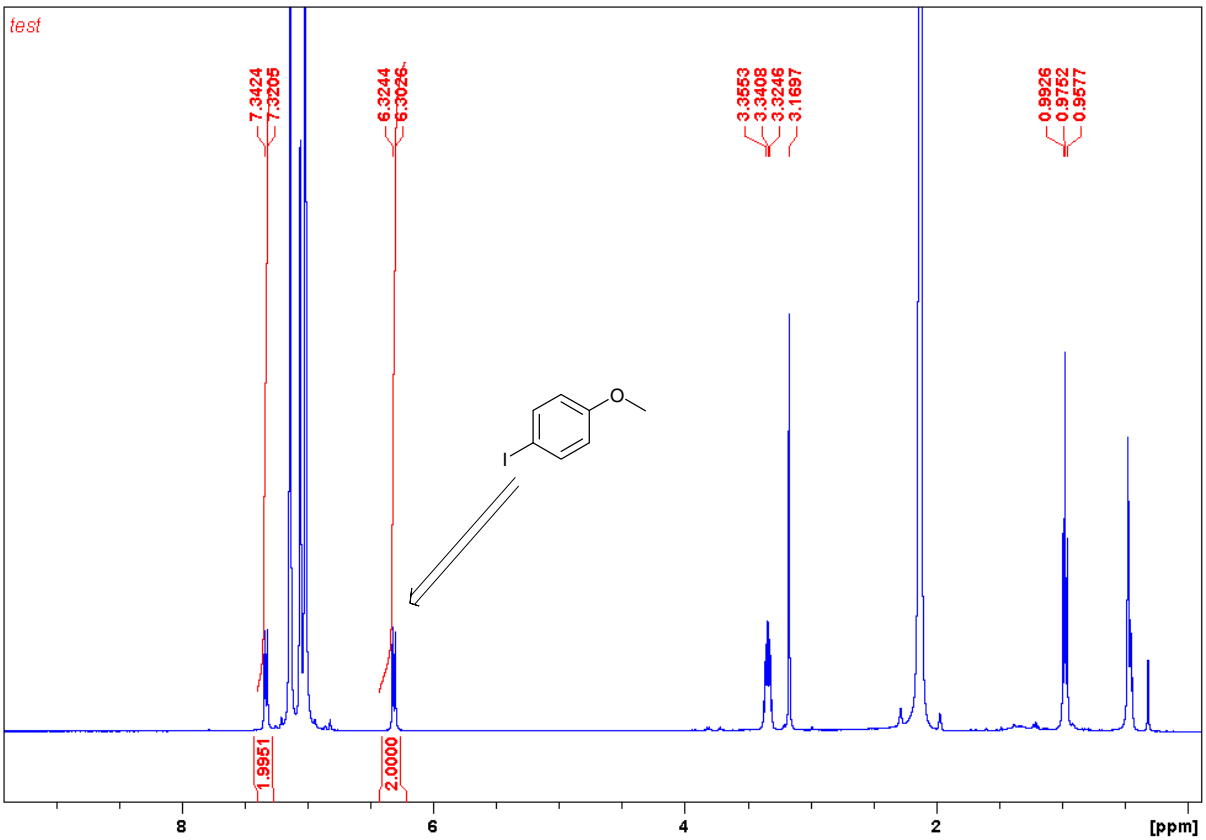

2.1 ^{1}H NMR spectrum (400 MHz, $CDCl_3$) of siloxane **11**

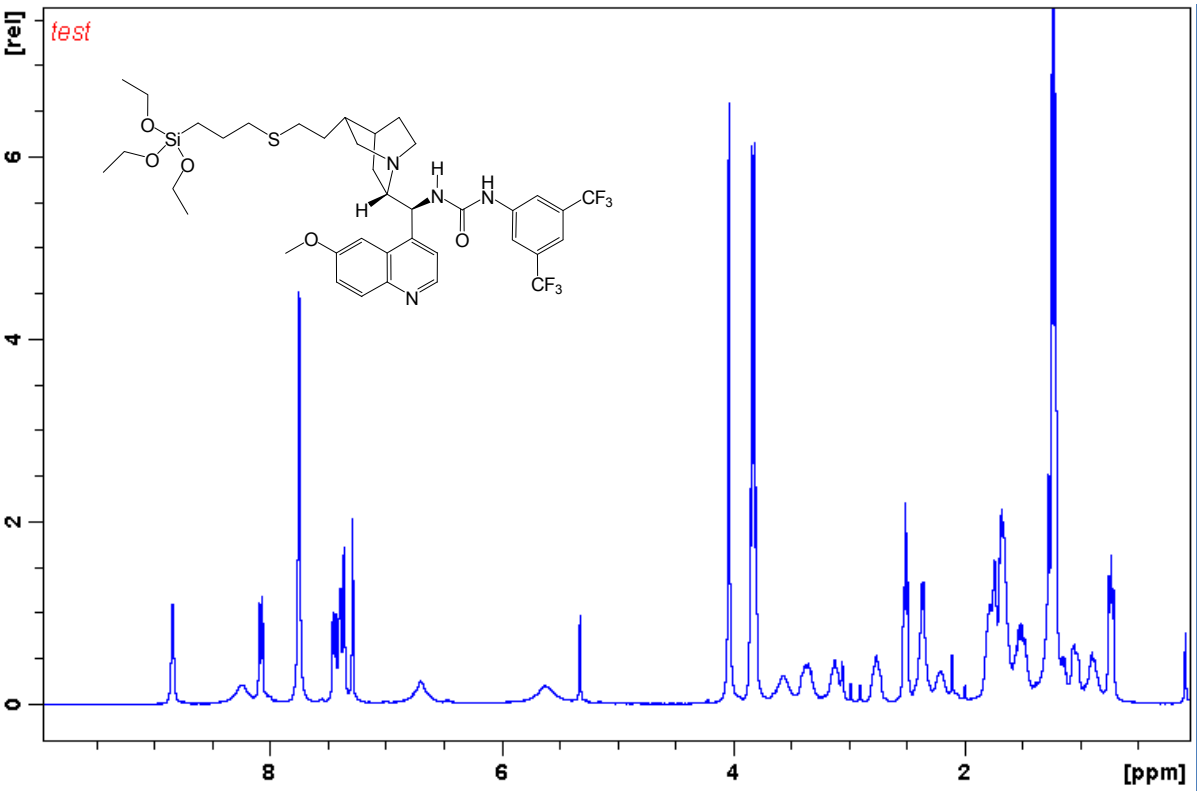

2.2 ^{13}C NMR spectrum (100 MHz, $CDCl_3$) of siloxane **11**

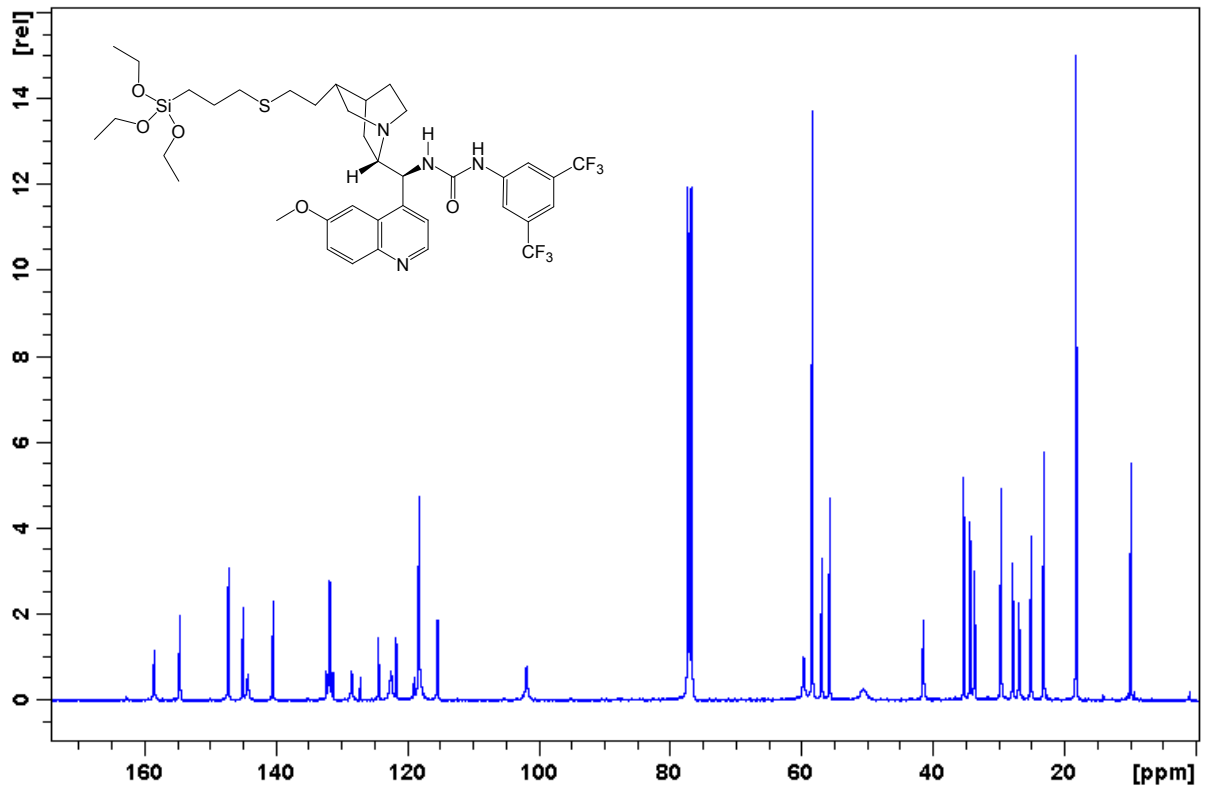

3.0 Evaluation of catalyst **8** in the addition of dimethyl malonate **13** to (*E*)-β-nitrostyrene **12**.

^{1}H NMR spectrum (400 MHz, $CDCl_3$) of the crude reaction mixture after 18 h.

Table 1, entry 1; 70% conversion.

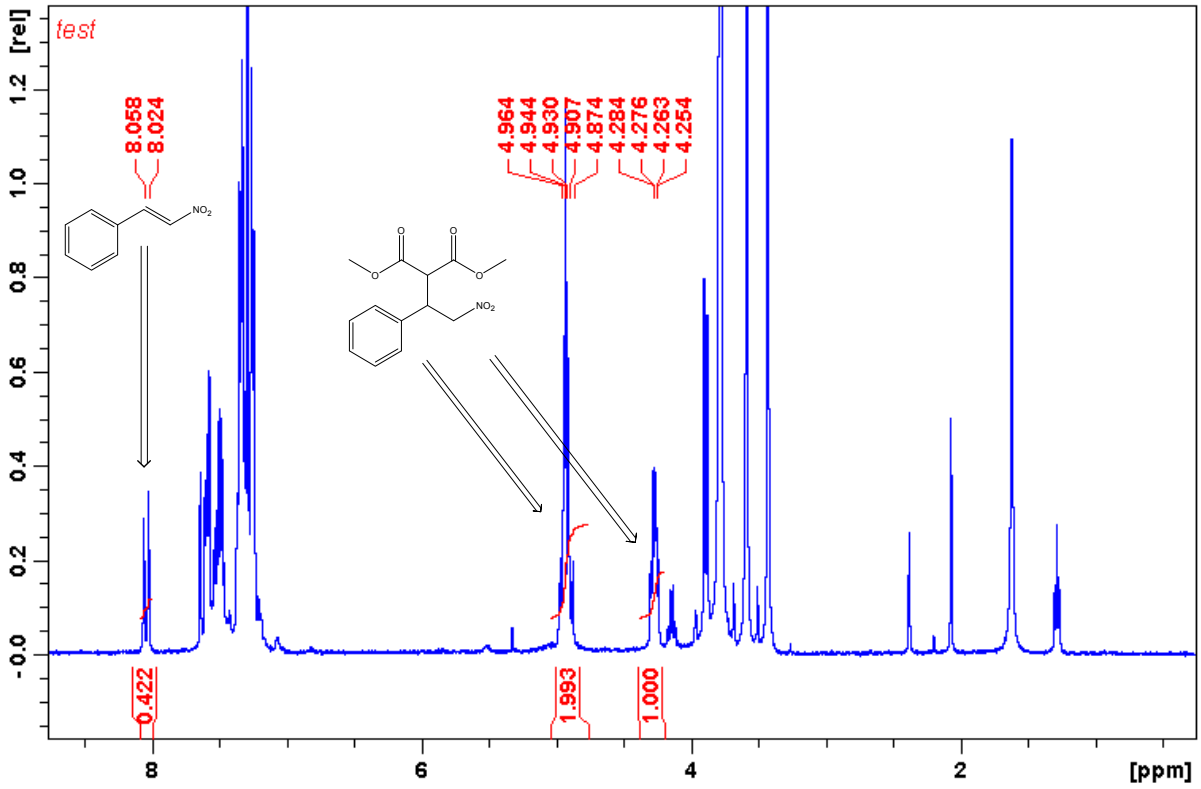

^{1}H NMR spectrum (400 MHz, $CDCl_3$) of the crude reaction mixture after 18 h.

Table 1, entry 2; 70% conversion.

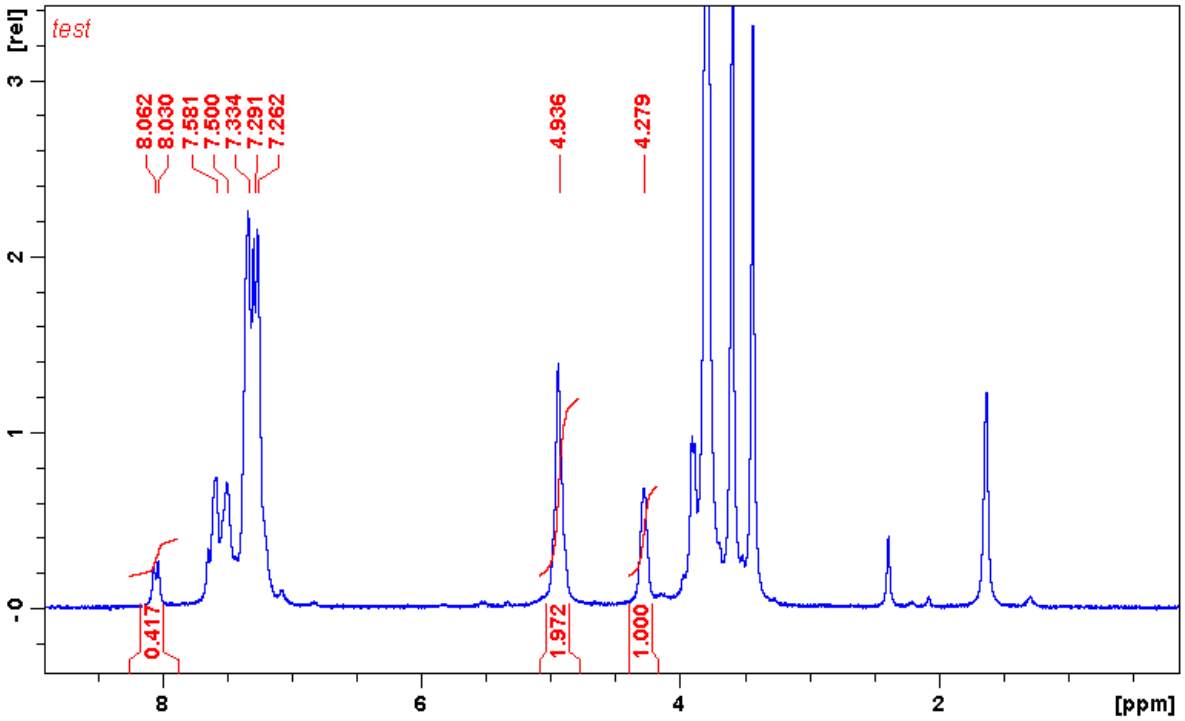

^{1}H NMR spectrum (400 MHz, $CDCl_3$) of the crude reaction mixture after 18 h.

Table 1, entry 3; 71% conversion.

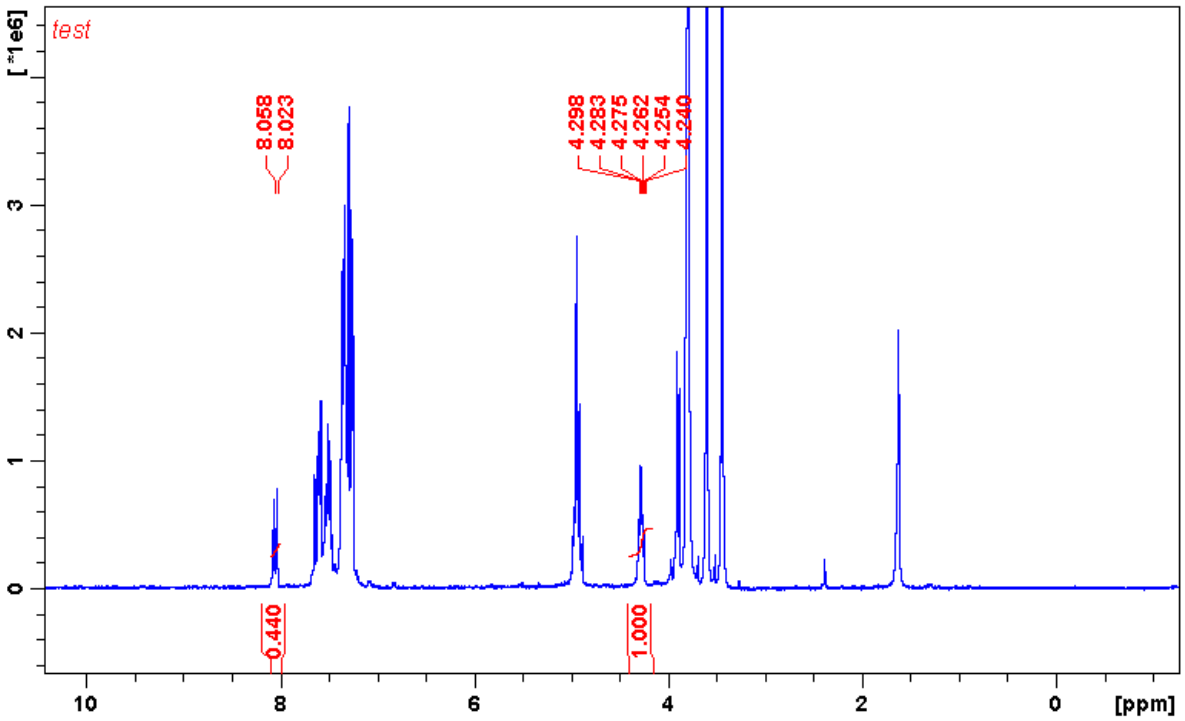

3.1 Enantiomeric excess determination by CSP-HPLC (Chiralcel AD-H (4.6 mm x 25 cm), Hexane/IPA: 9/1, 1.0 mL min^{-1}, RT, UV 220 nm) analysis of the recovered dimethyl 2-(2-nitro-1-phenylethyl)malonate **14**

Table 1, entry 1; 71% *ee*

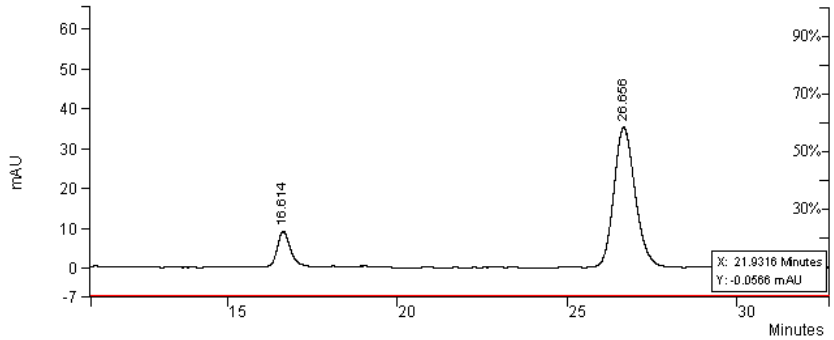

Time (min)	Result %
16.6	10.8306
26.7	60.3788

Enantiomeric excess determination by CSP-HPLC (Chiralcel AD-H (4.6 mm x 25 cm), Hexane/IPA: 9/1, 1.0 mL min^{-1}, RT, UV 220 nm) analysis of the recovered dimethyl 2-(2-nitro-1-phenylethyl)malonate **14**

Table 1, entry 2; 72% *ee*

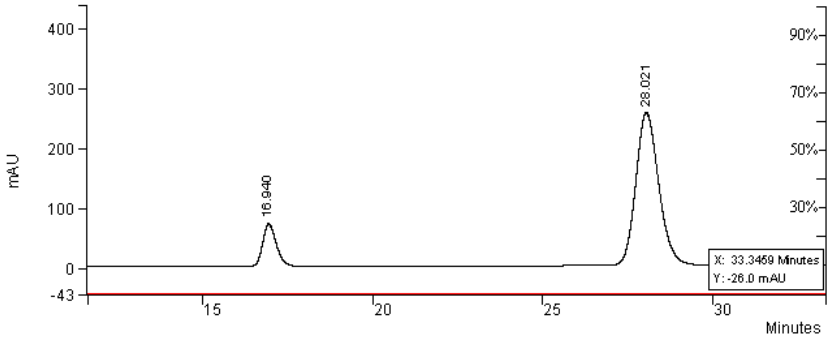

Time (min)	Result %
16.9	10.9009
28.0	65.8699

Enantiomeric excess determination by CSP-HPLC (Chiralcel AD-H (4.6 mm x 25 cm), Hexane/IPA: 9/1, 1.0 mL min^{-1}, RT, UV 220 nm) analysis of the recovered dimethyl 2-(2-nitro-1-phenylethyl)malonate **14**

Table 1, entry 3; 77% *ee*

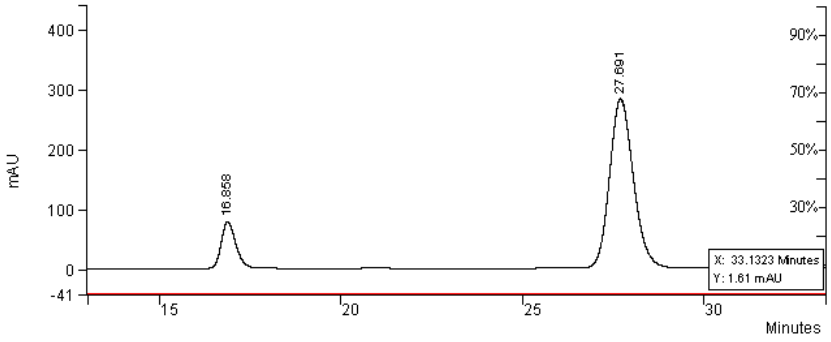

Time (min)	Result %
16.9	10.6433
27.7	79.5213

4.0 Characterisation of **24**

4.1 FTIR analysis

The FTIR spectra for the magnetite nanoparticles before and after loading with the sulfonamide catalyst to form compound **24** are shown in **Figure 4**. The spectrum for magnetite nanoparticles alone (black line) shows a stretching vibration at 3440 cm^{-1} which incorporates the contributions from both symmetrical (v_1) and asymmetrical (v_3) modes of the O-H bonds which are attached to the surface iron atoms. The presence of an adsorbed water layer is confirmed by a stretch for the vibrational mode of water found at 1635 cm^{-1}. The absorption band at 581 cm^{-1} is attributed to Fe-O bonds of the magnetite nanoparticles. In the spectrum for the catalyst-loaded nanoparticles, **24**, additional stretches at 2870, 2005, 1758, 1420, 1203, 1141 and 1034 cm^{-1} are noted, representing the various organic functionalities of the sulfonamide group.

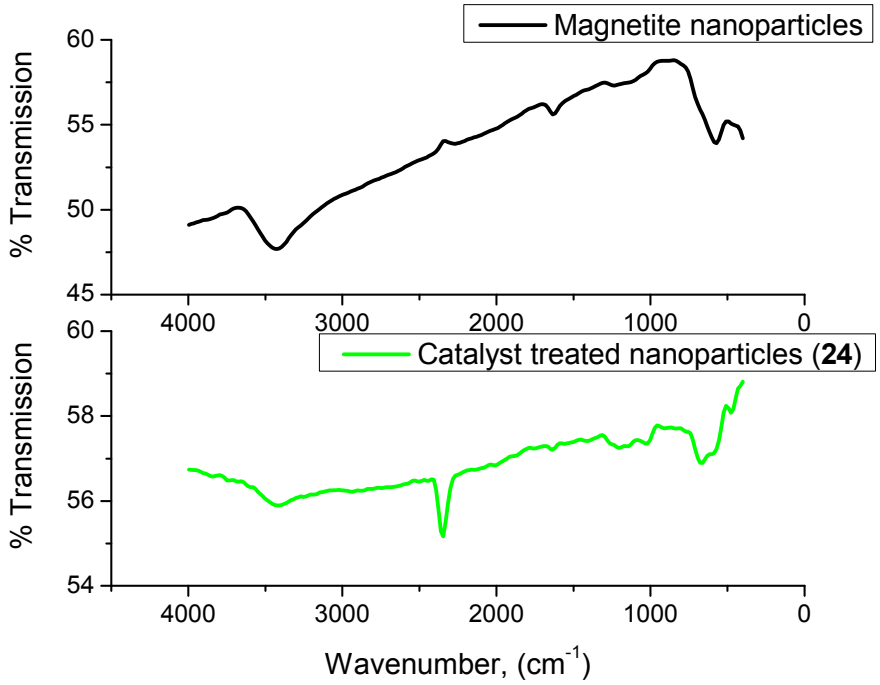

Figure 4. FTIR spectra of magnetite nanoparticles (black) and sulphonamide catalyst-loaded nanoparticles (**24**) (green).

4.2 TGA studies

TGA was carried out on the magnetite nanoparticles before and after loading with the sulfonamide catalyst for form compound **24** (**Figure 5**). The total weight loss from the magnetite nanoparticles alone is 2%. Much of this small weight percentage loss is due to the loss of strongly adsorbed water and surface hydroxyl groups from the particles which takes place between 30 and 250 ^{o}C. Slight changes in the curve after 500 ^{o}C are due to a phase change of the material from magnetite to maghemite. The curve representing the catalyst-loaded magnetite nanoparticles shows a total weight loss of 8%. Above 200 ^{o}C, organic groups representative of the functionalised catalyst are desorbed from the nanoparticles. This confirms the functionalisation of the nanoparticles with the catalyst, as expected.

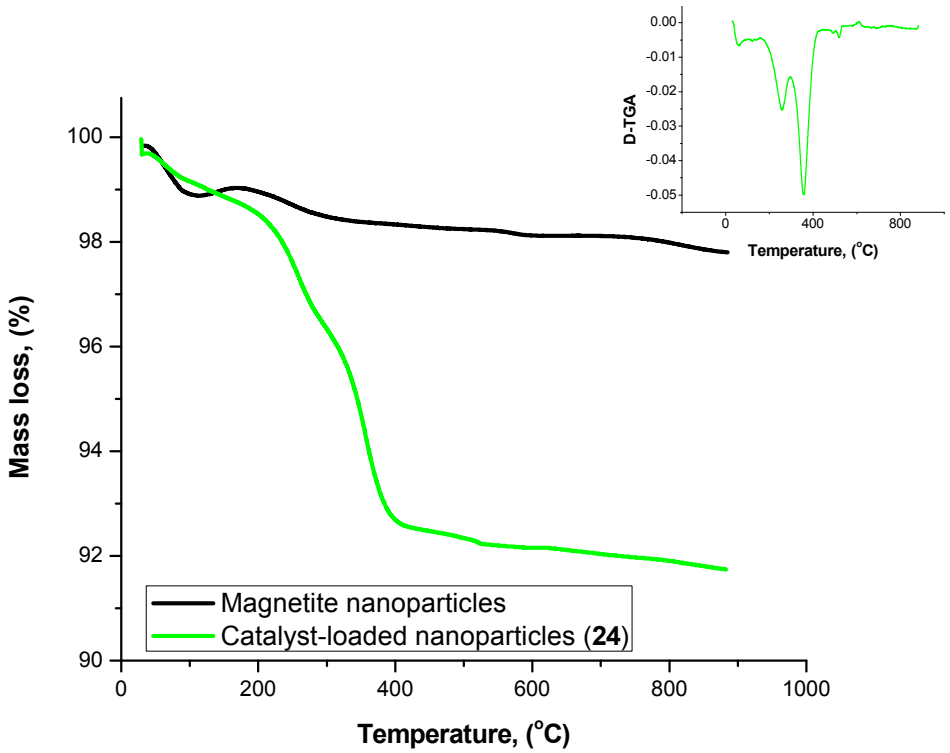

Figure 5. TGA curves of percentage mass lost on heating from 30-900 °C of magnetite nanoparticles (black) and sulphonamide catalyst-loaded nanoparticles (**24**) (green).

4.3 XRD studies

A dry solid powder sample was used to collect XRD patterns of the sample of magnetite nanoparticles and the sulphonamide catalyst-loaded nanoparticles (**Figure 6**). The observed patterns both correspond well to the JCPDS database for magnetite. The average particle size has been calculated from the peak width at half maximum of the peak at 35.5 degrees 2θ, using the Debye-Scherrer equation.[1] The average particle size was found to be 10.57 nm, which is in close agreement with the particle size as calculated from TEM. The calculated size was the same for the magnetite before and after loading with catalyst. The interlayer spacings (d_{hkl}), calculated using the Bragg equation, agree well with the data for standard magnetite (**Table 1**). The *a* lattice parameter was calculated as 0.840 nm, which coincides closely with the value for magnetite (0.839 nm). The peaks at 12.2 and 74 degrees 2θ appear due to the lamp present in the XRD machine. The peak at 23 degrees 2θ is due to the silica gel used to adhere the sample to the glass holder.

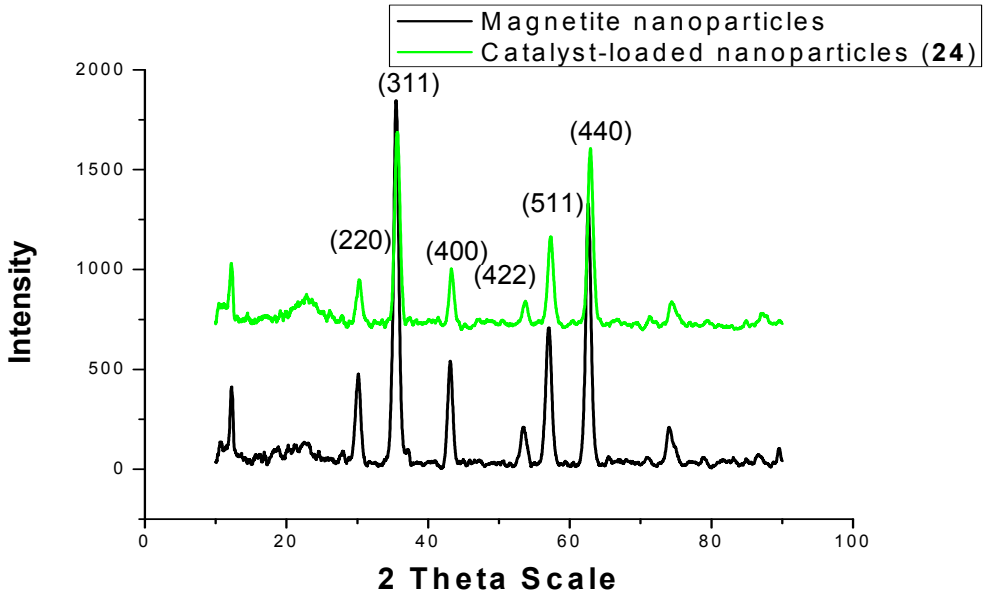

Figure 6. XRD patterns of magnetite nanoparticles (black) and sulphonamide catalyst-loaded nanoparticles (**24**) (green).

5.0 NMR spectra of siloxane **25** and determination of its loading by ^{1}H NMR spectroscopy

^{1}H NMR spectrum (600 MHz, $CDCl_3$) of siloxane **25**

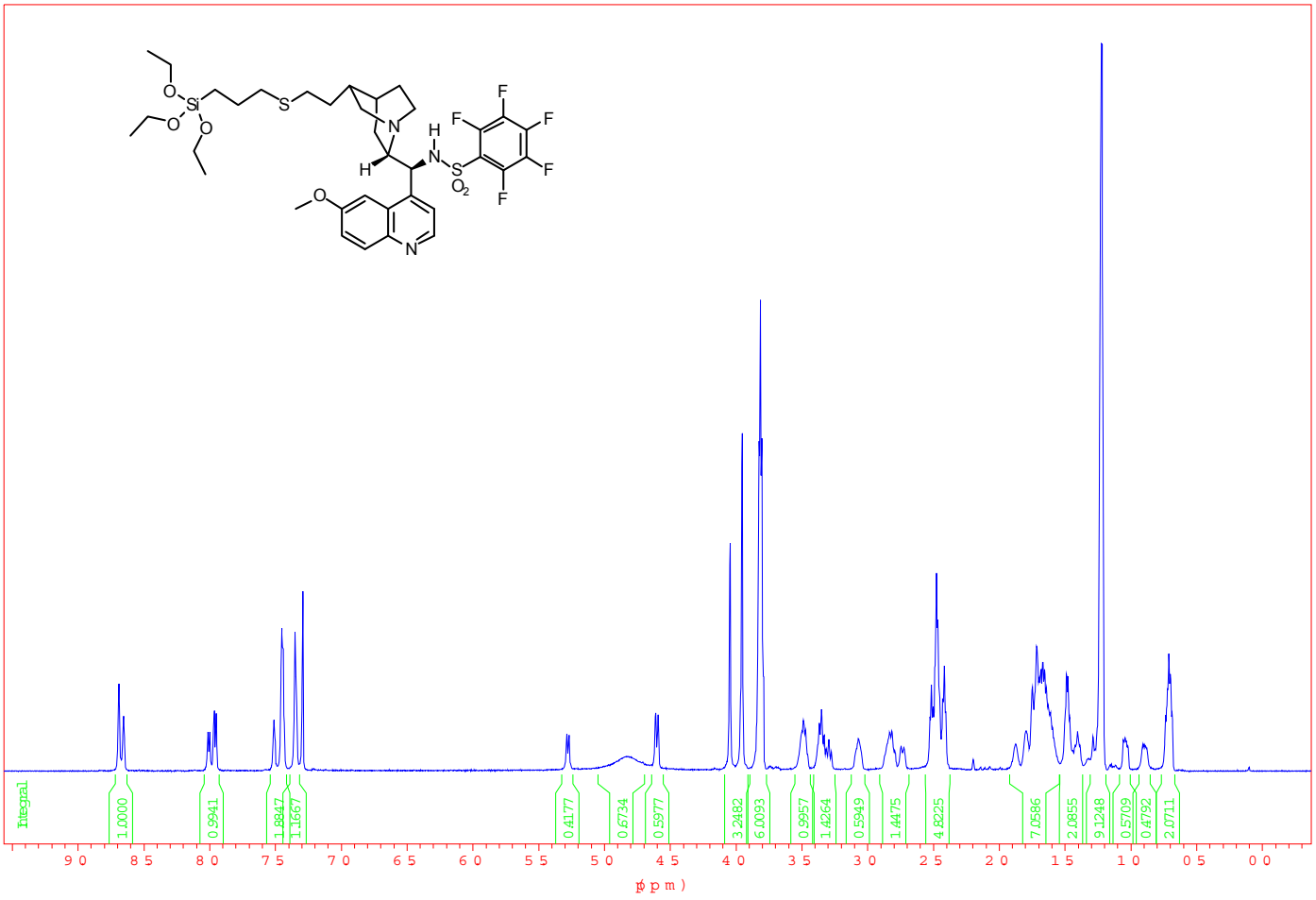

^{13}C NMR spectrum (150 MHz, $CDCl_3$) of siloxane **25**

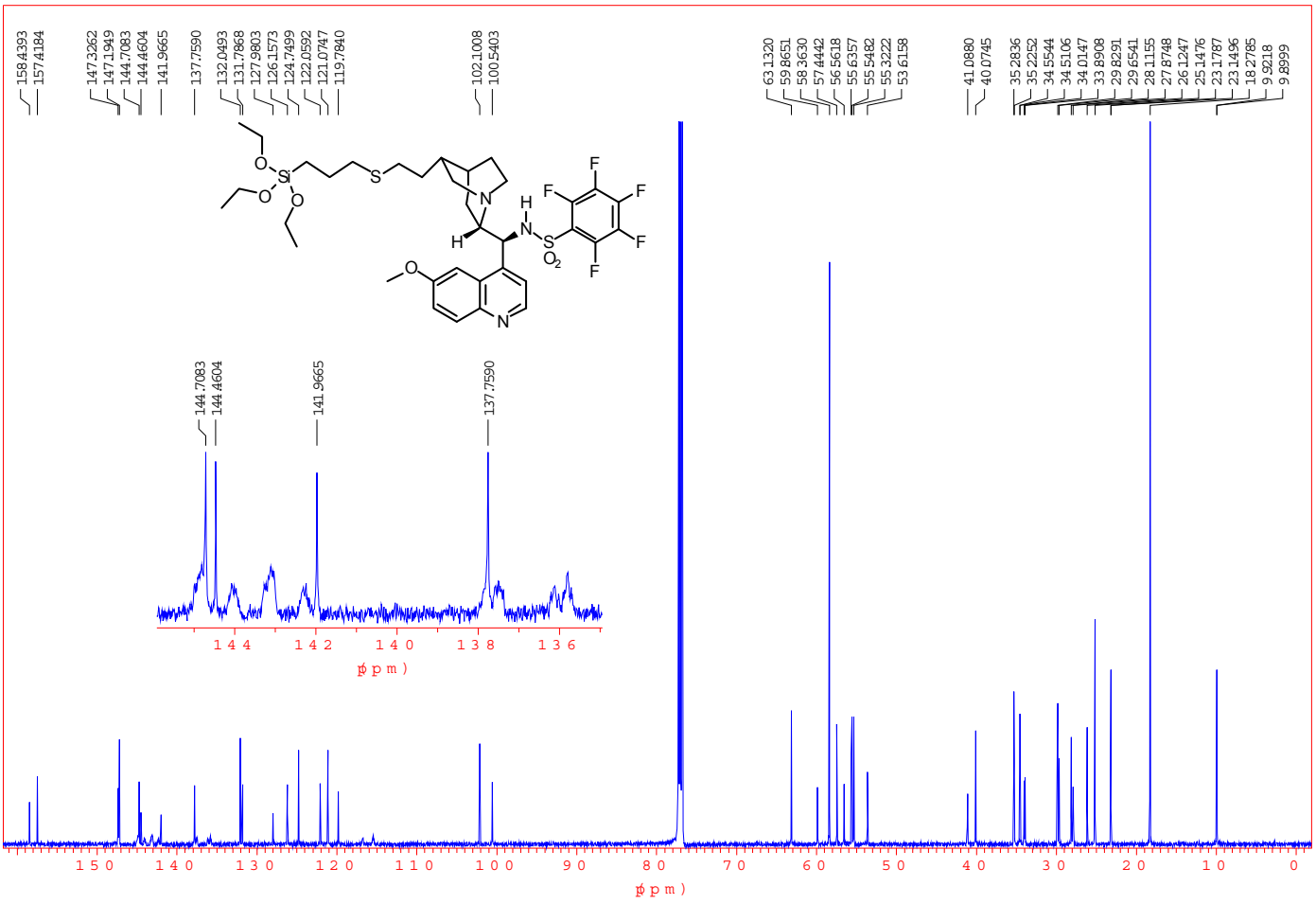

Determination of catalyst **(25)** loading by ^{1}H NMR spectroscopic analysis

The integration of the material to be loaded is compared to that of the 2,5-diphenyl furan (internal standard) both before (t = 0) and after 24 h. No traces of loading precursor (**25**) could be detected in the ^{1}H NMR spectrum of the reaction mixture after 24 h stirring. Loading: 1.00 mmol g^{-1}.

^{1}H NMR spectrum (400 MHz, $CDCl_3$) at t = 0

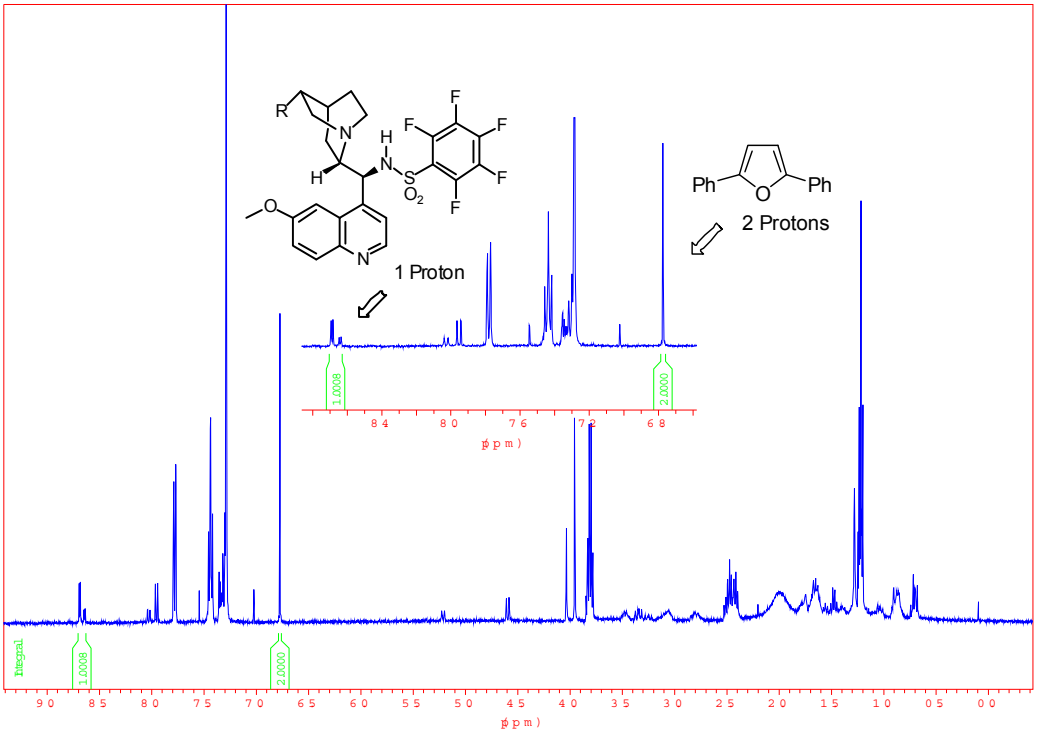

^{1}H NMR spectrum (400 MHz, $CDCl_3$) at t = 24 h.

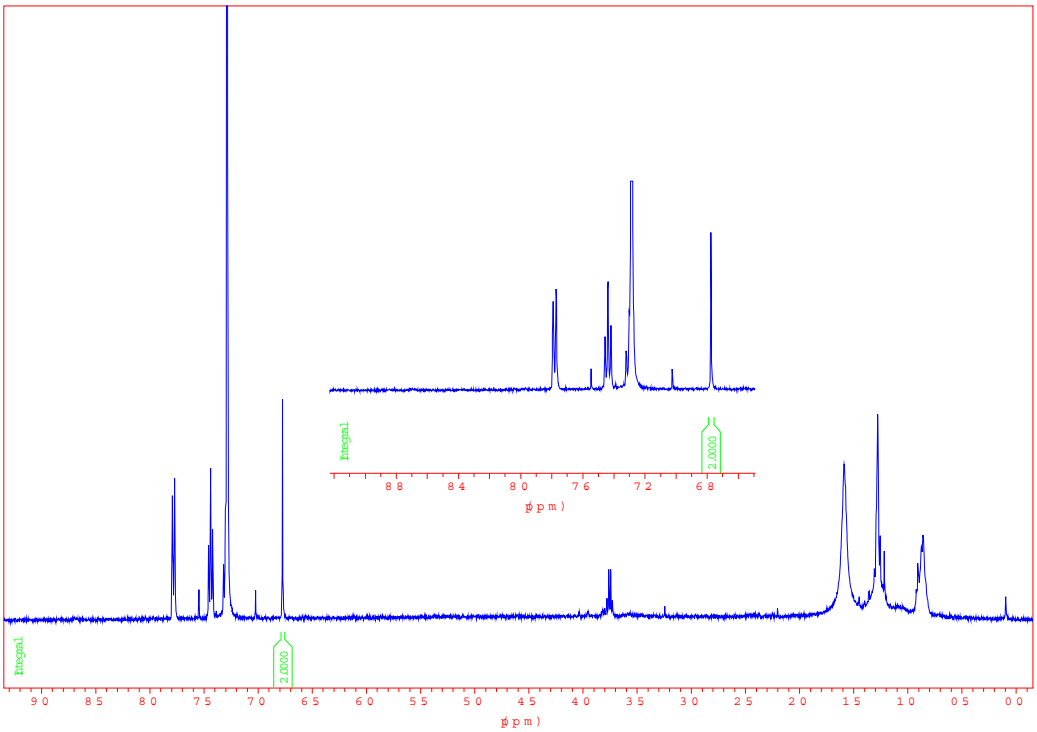

6.0 Evaluation of **24** as a recyclable catalyst in the desymmetrisation of anhydride **20** (Table 5)

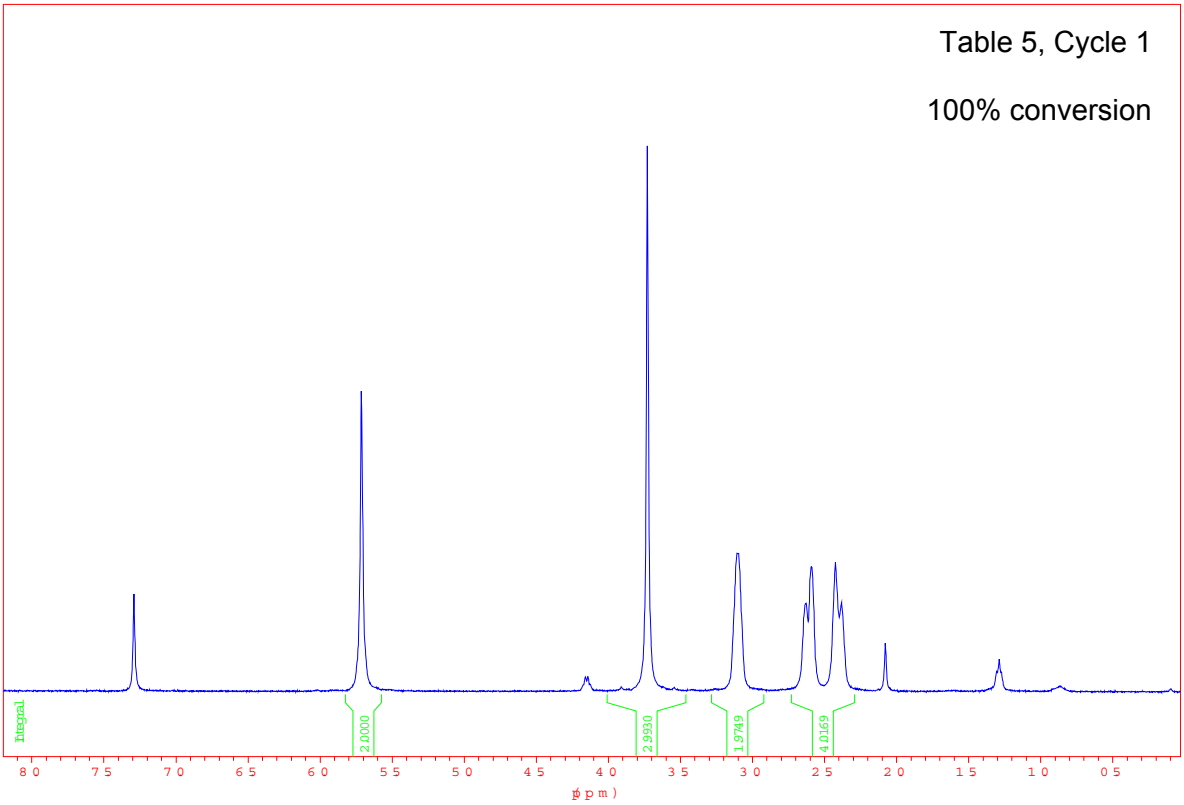

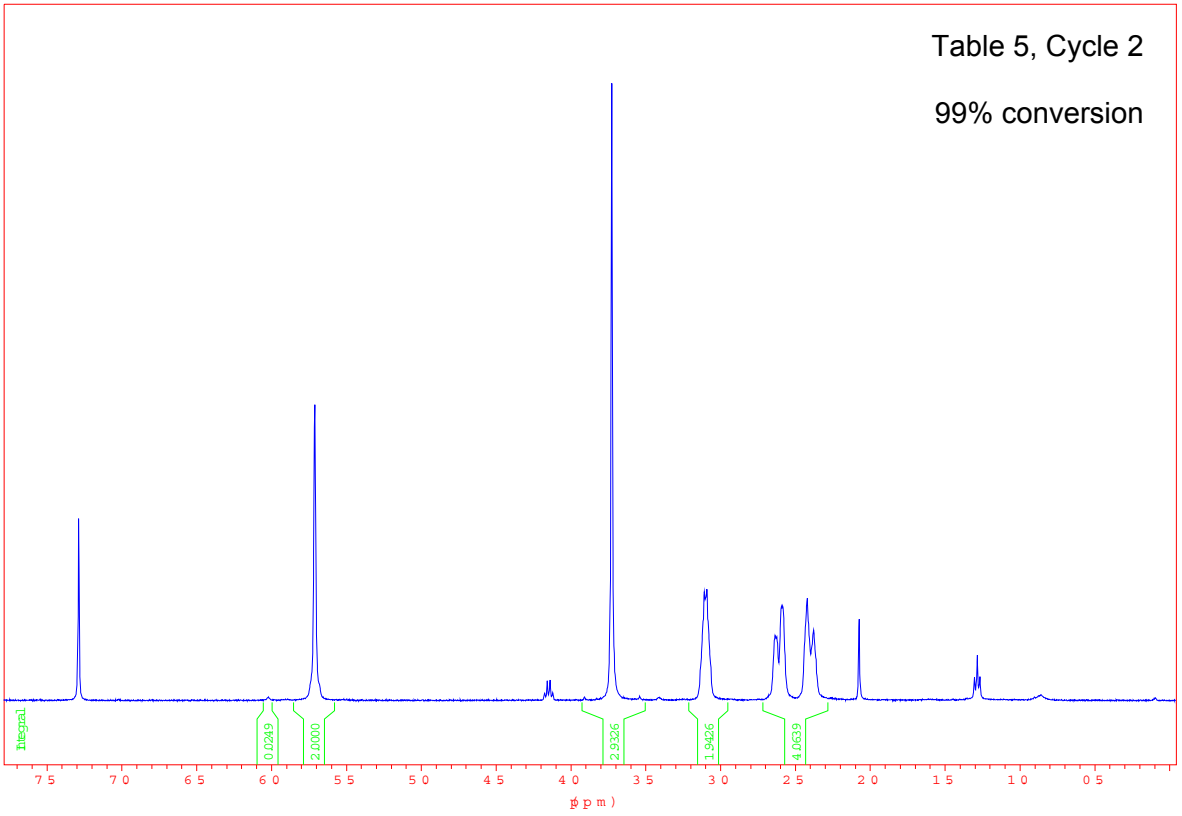

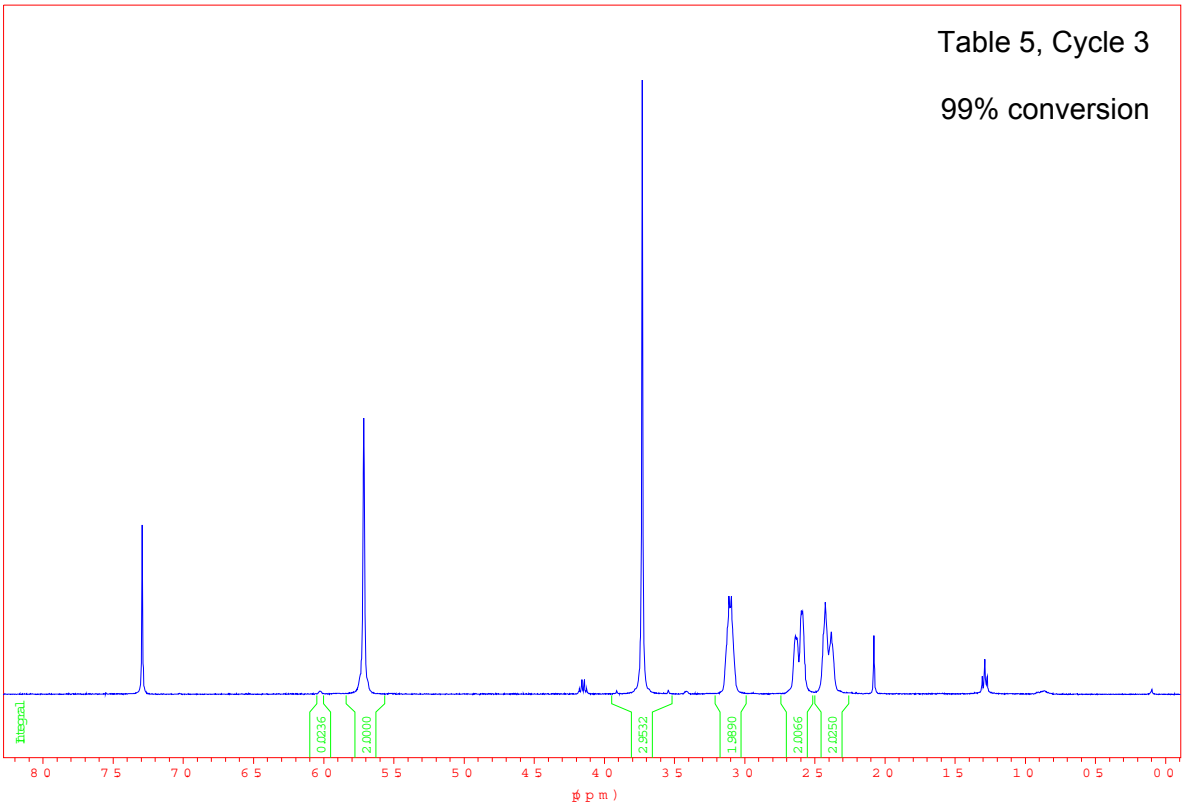

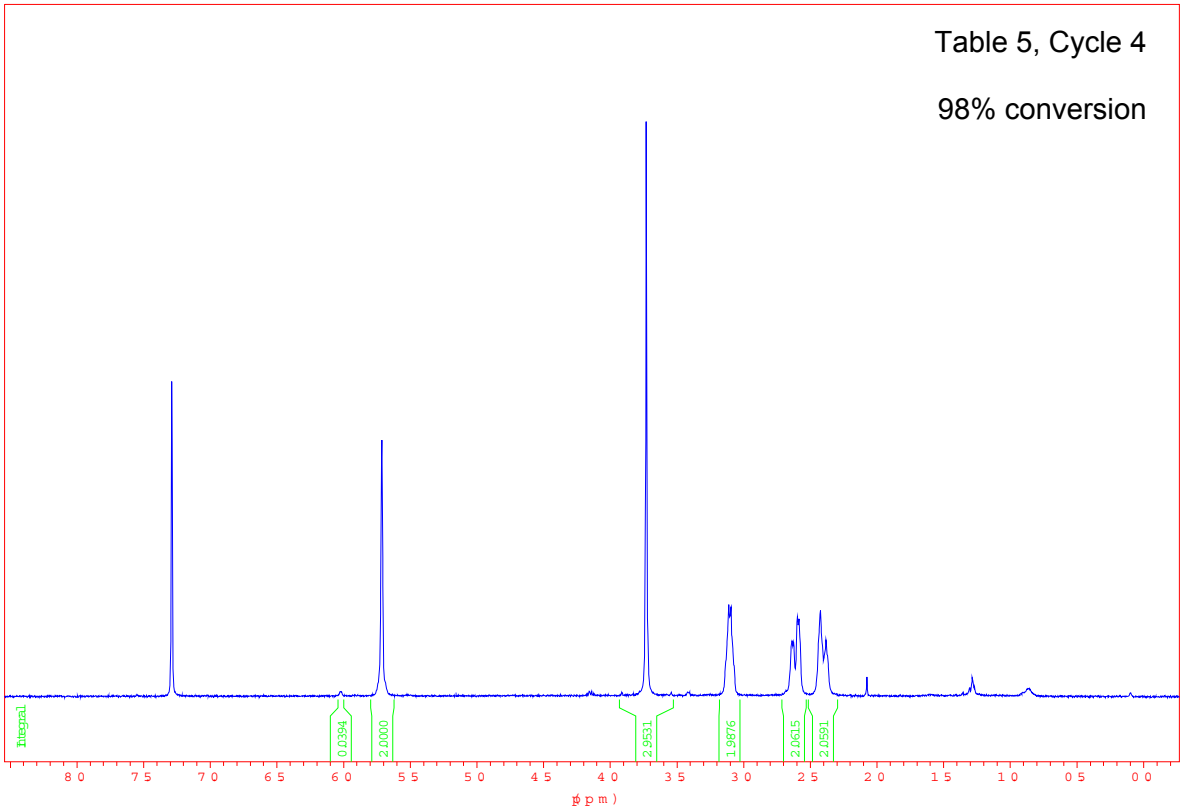

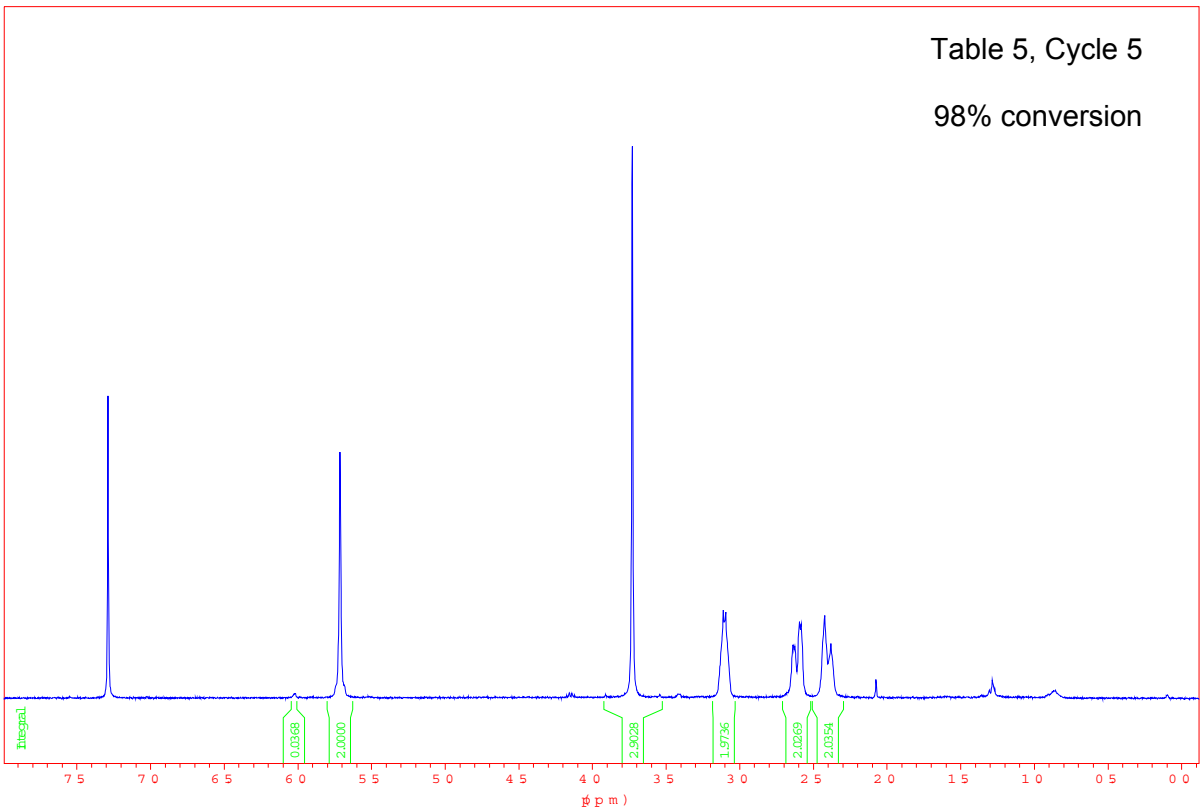

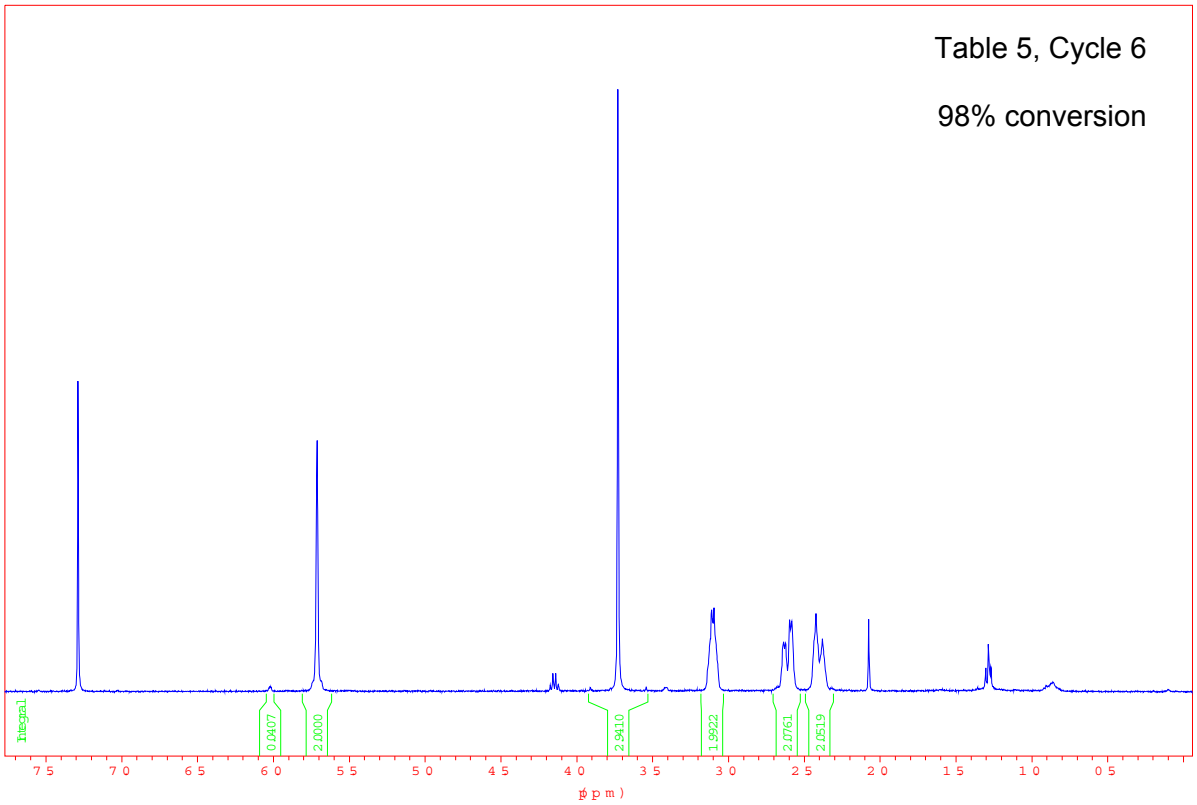

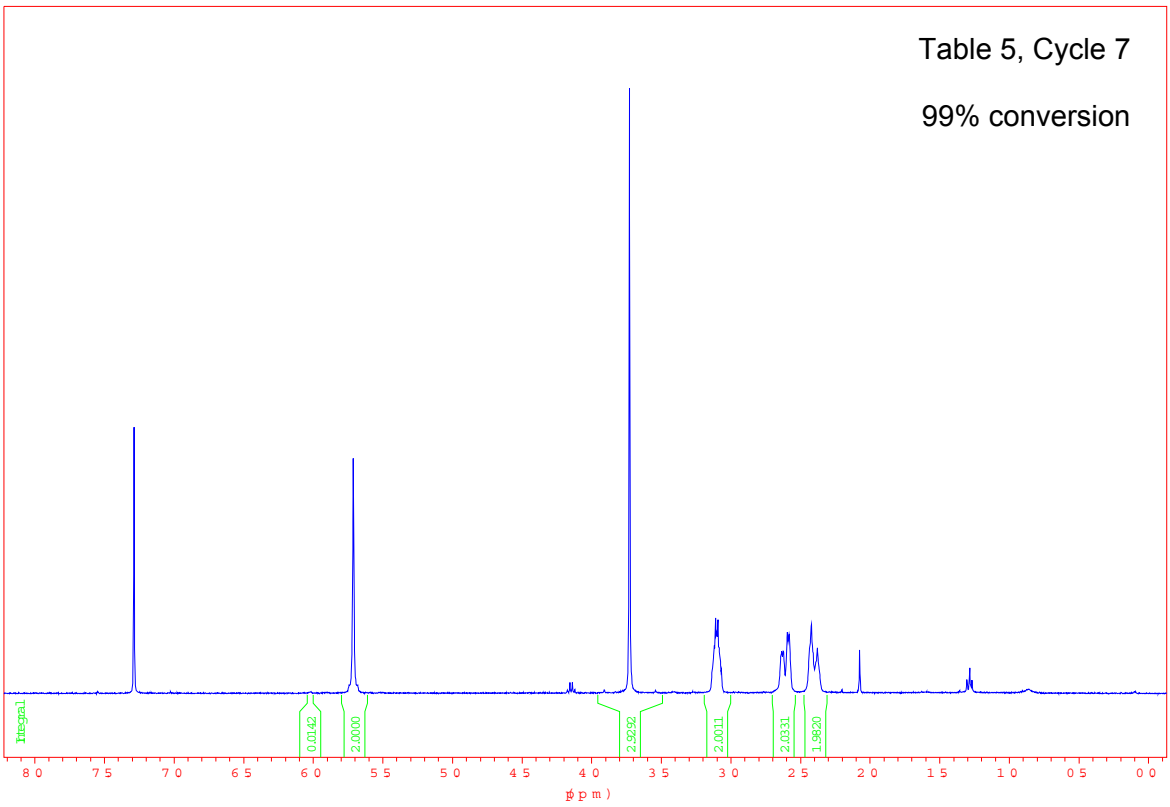

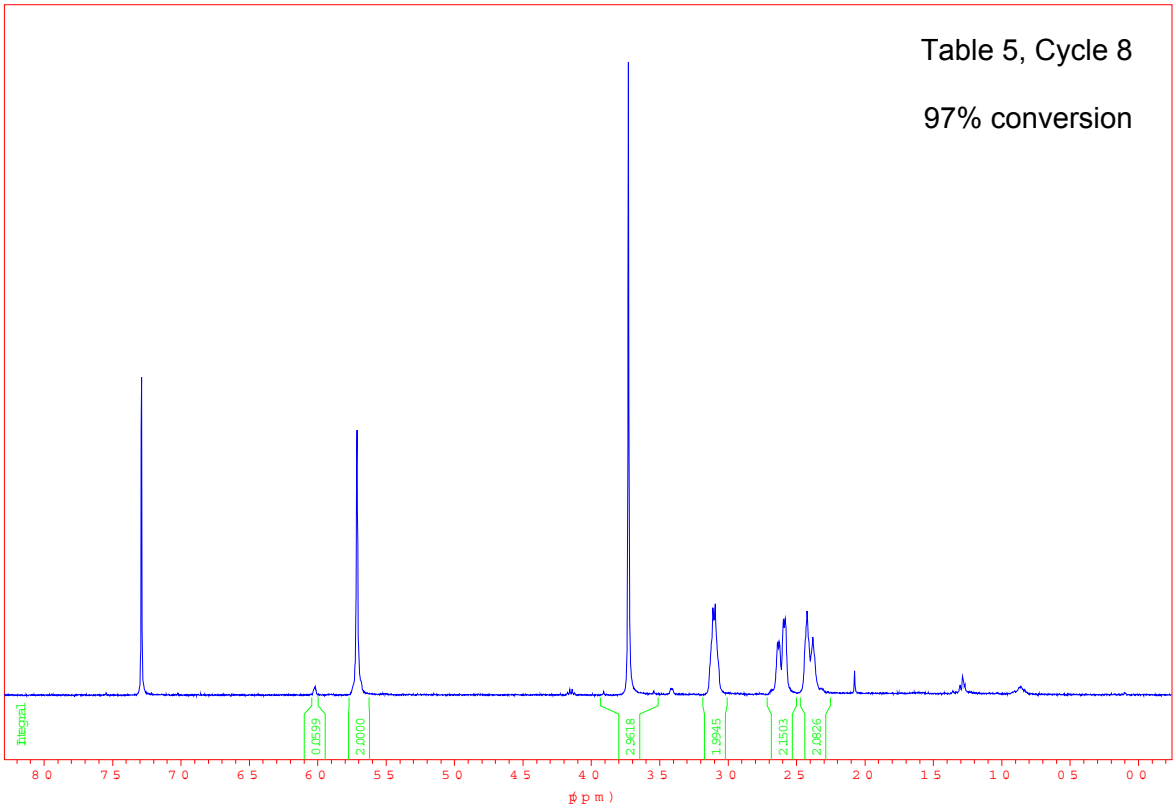

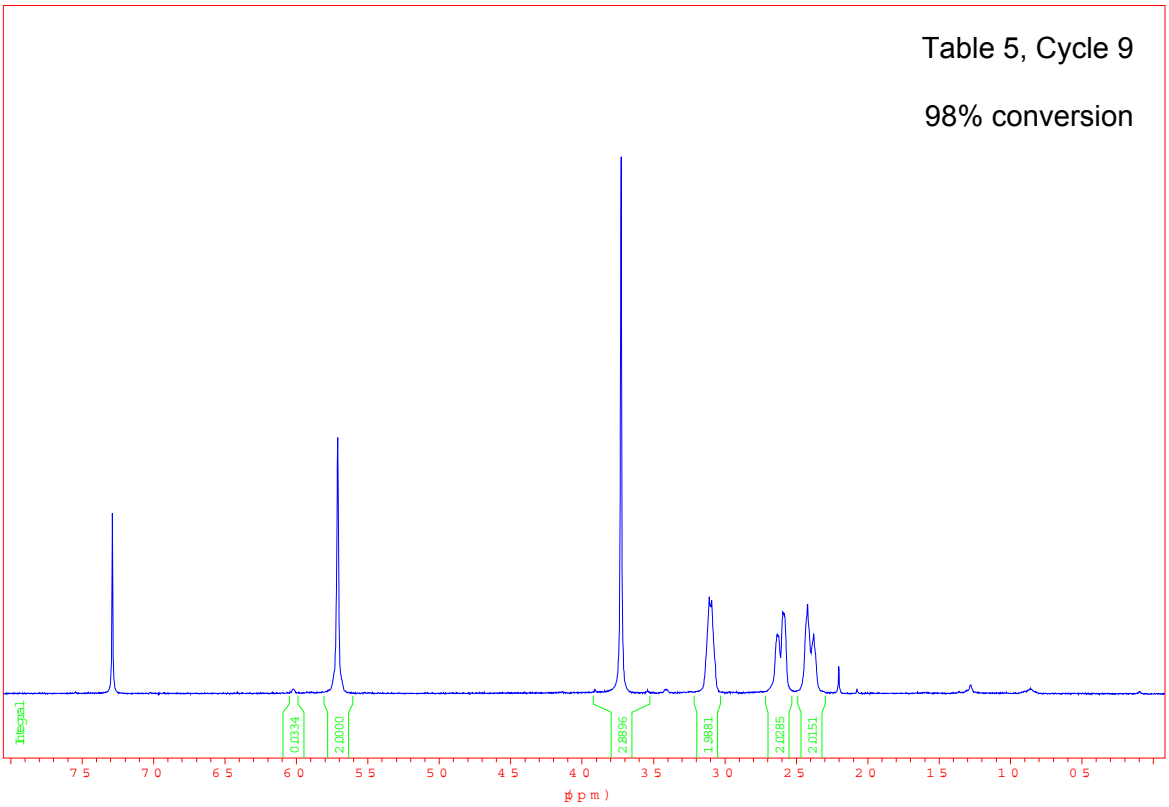

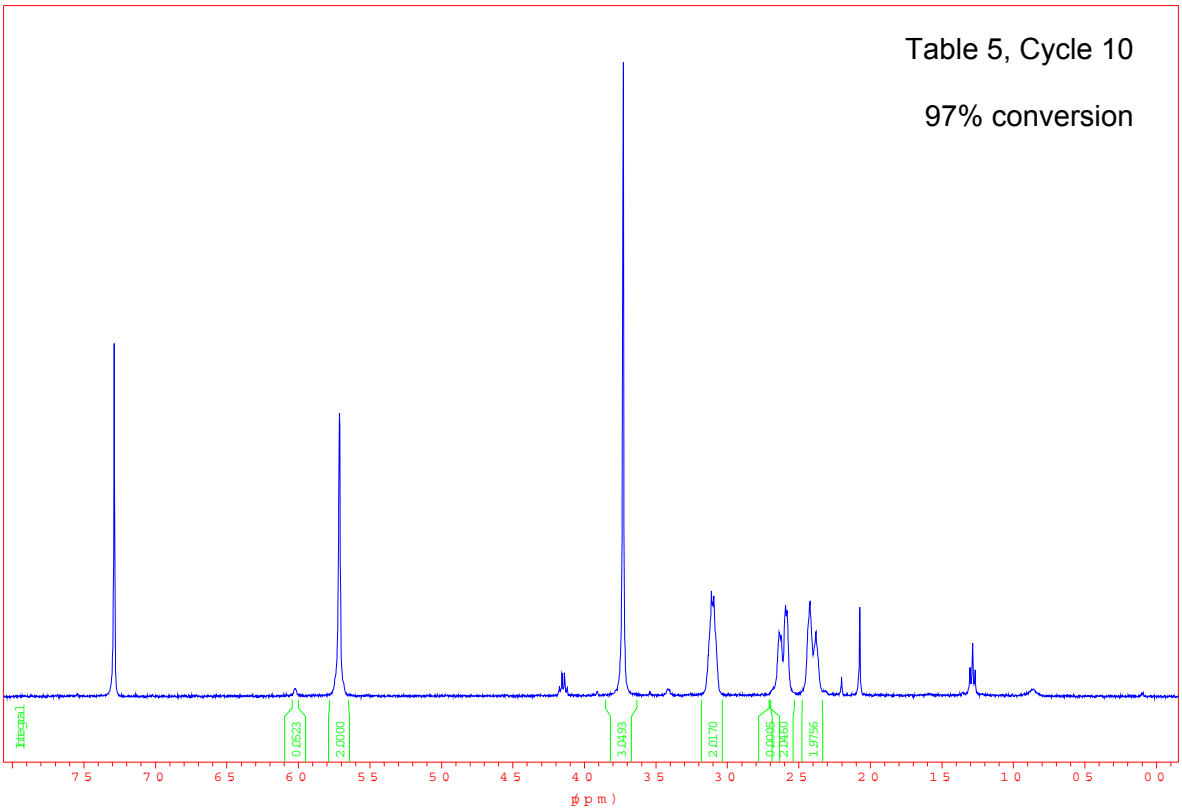

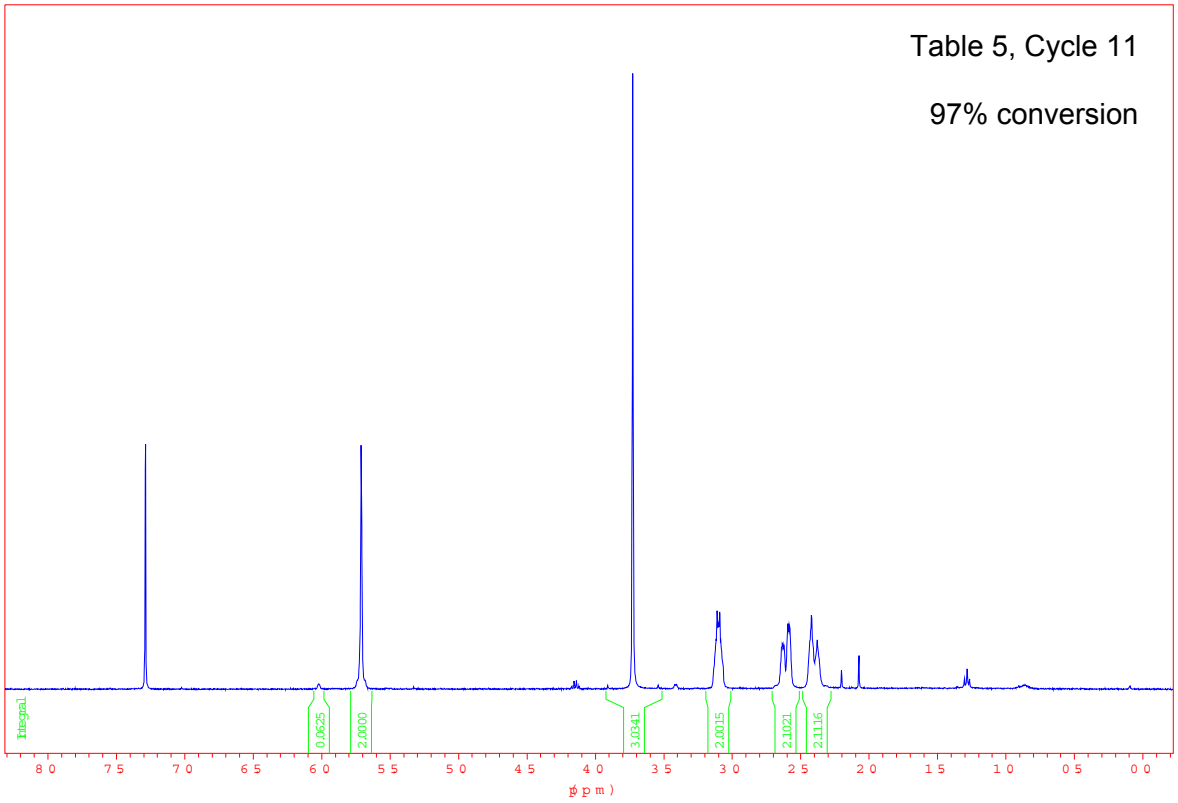

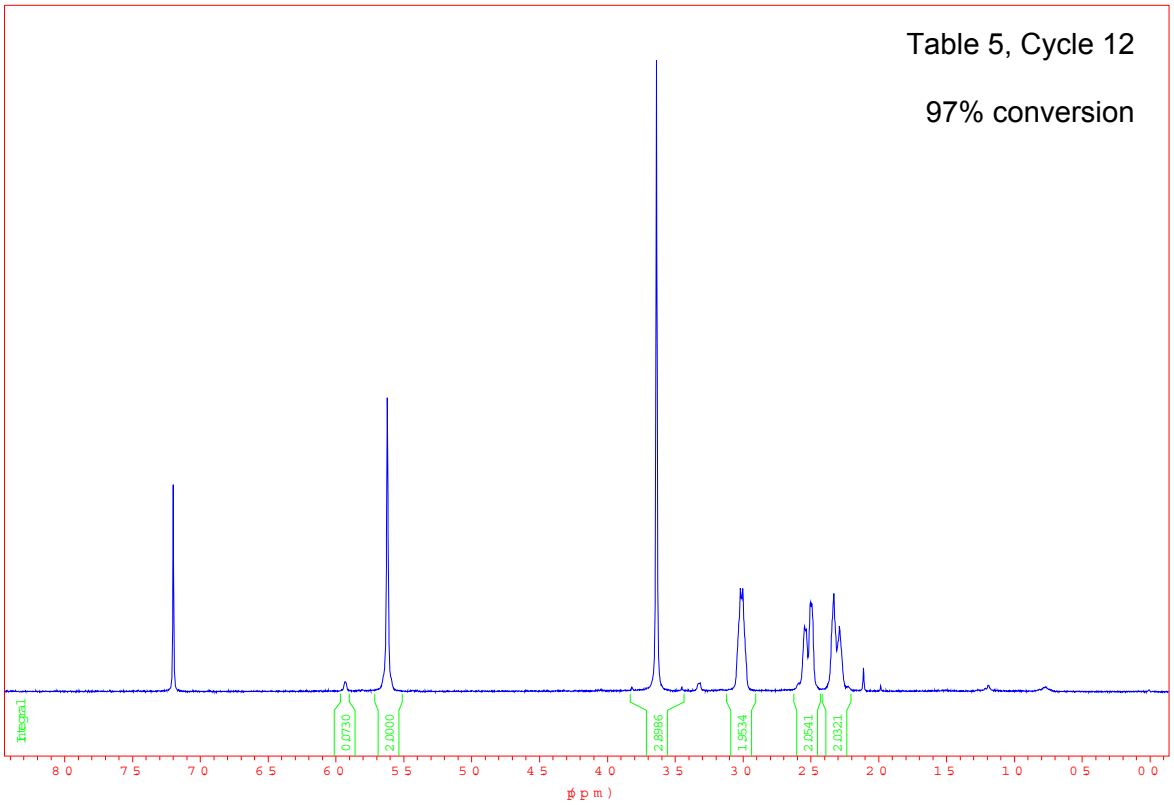

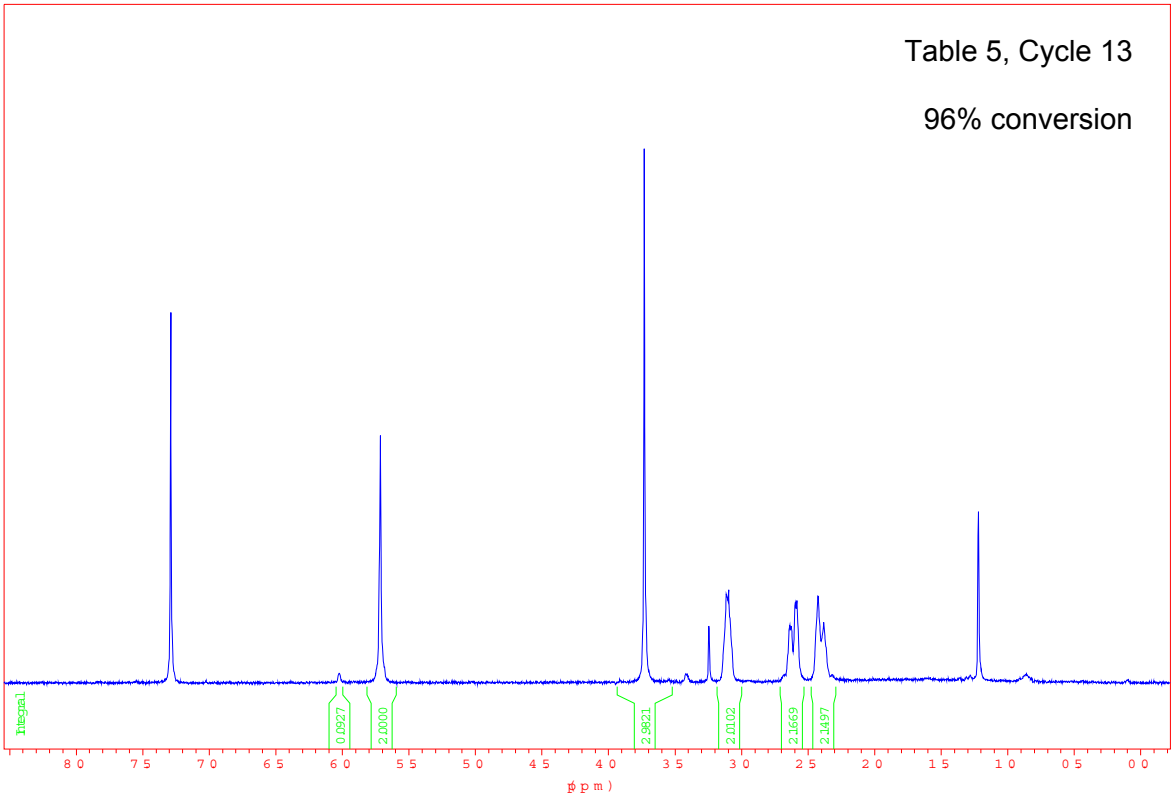

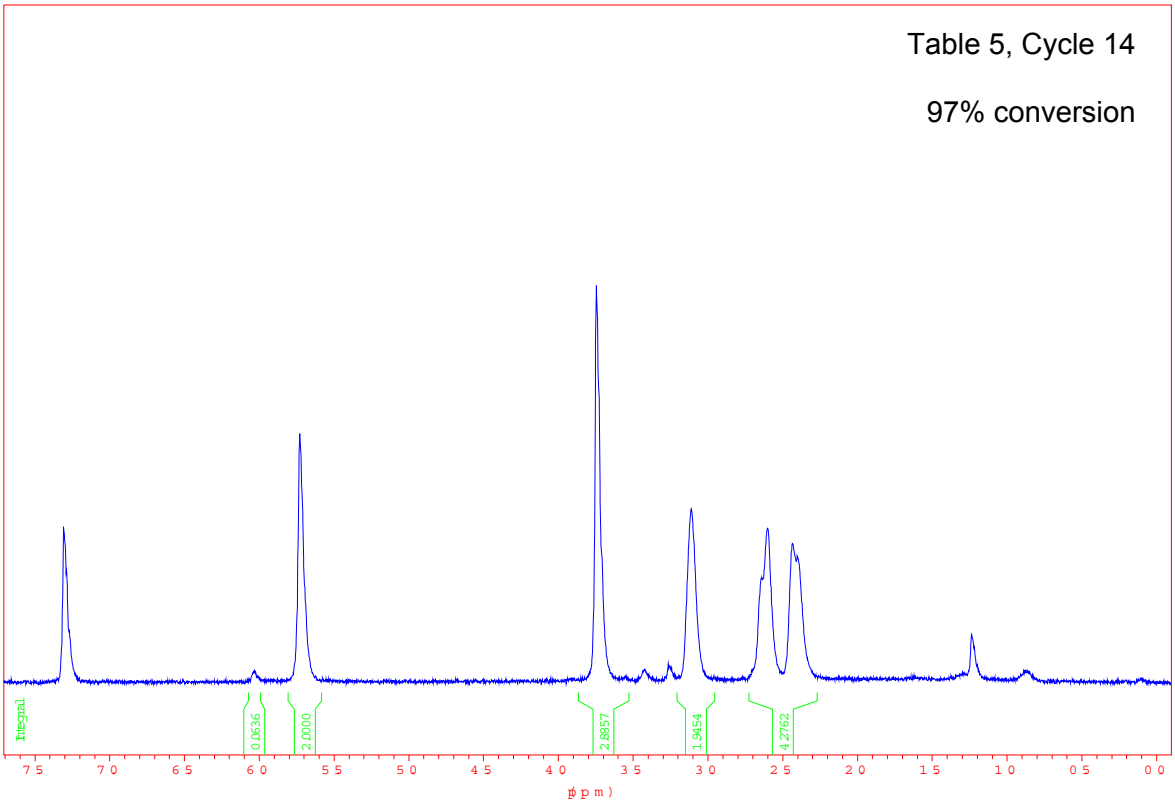

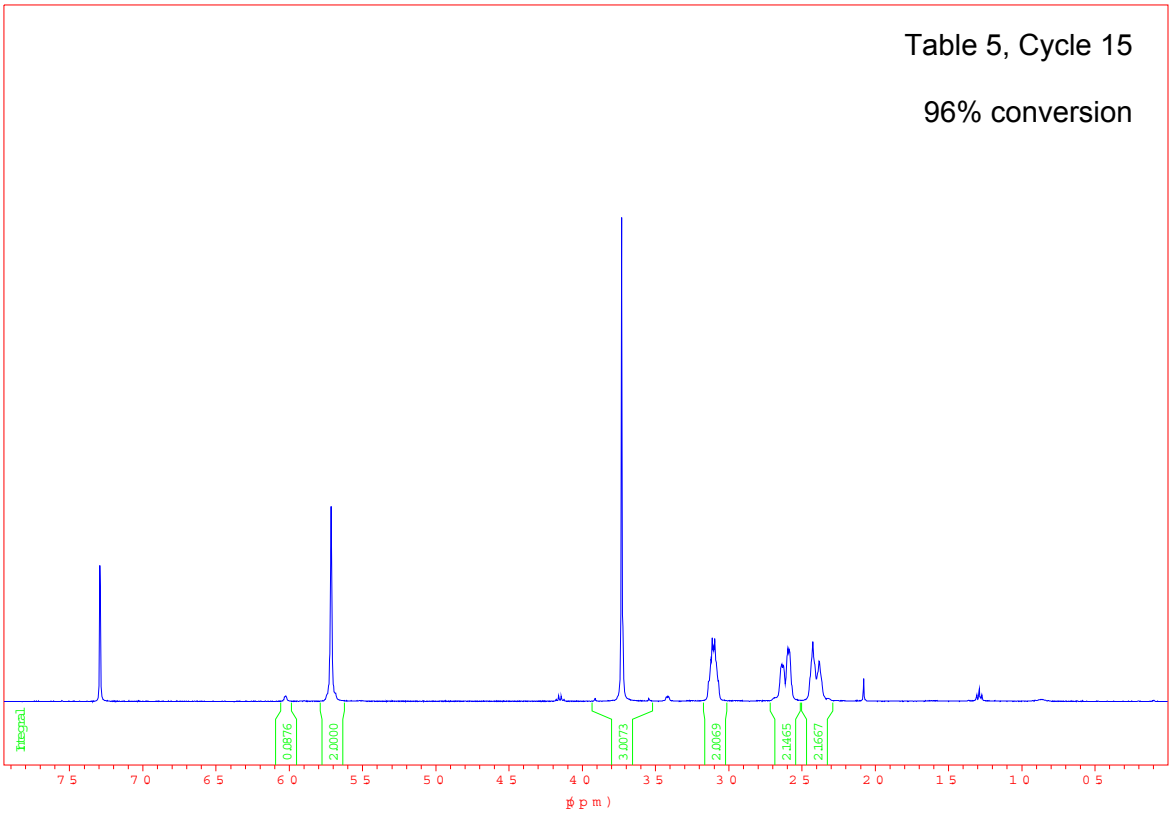

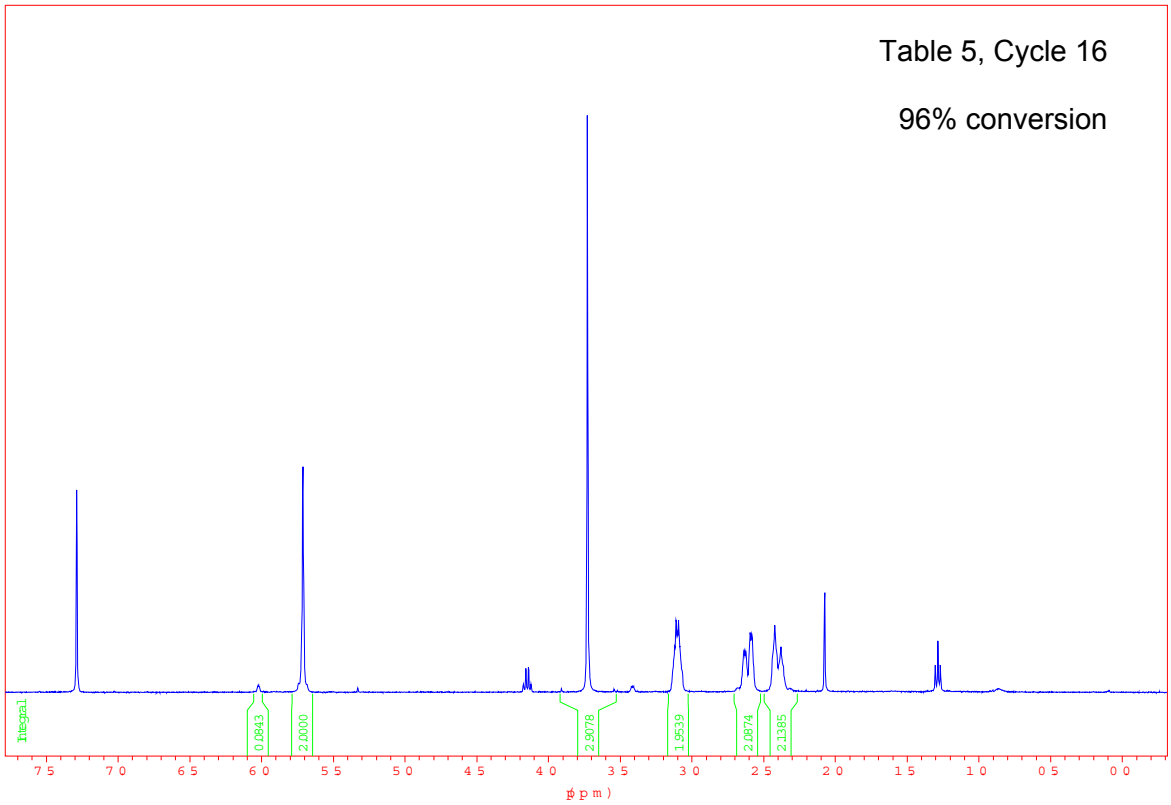

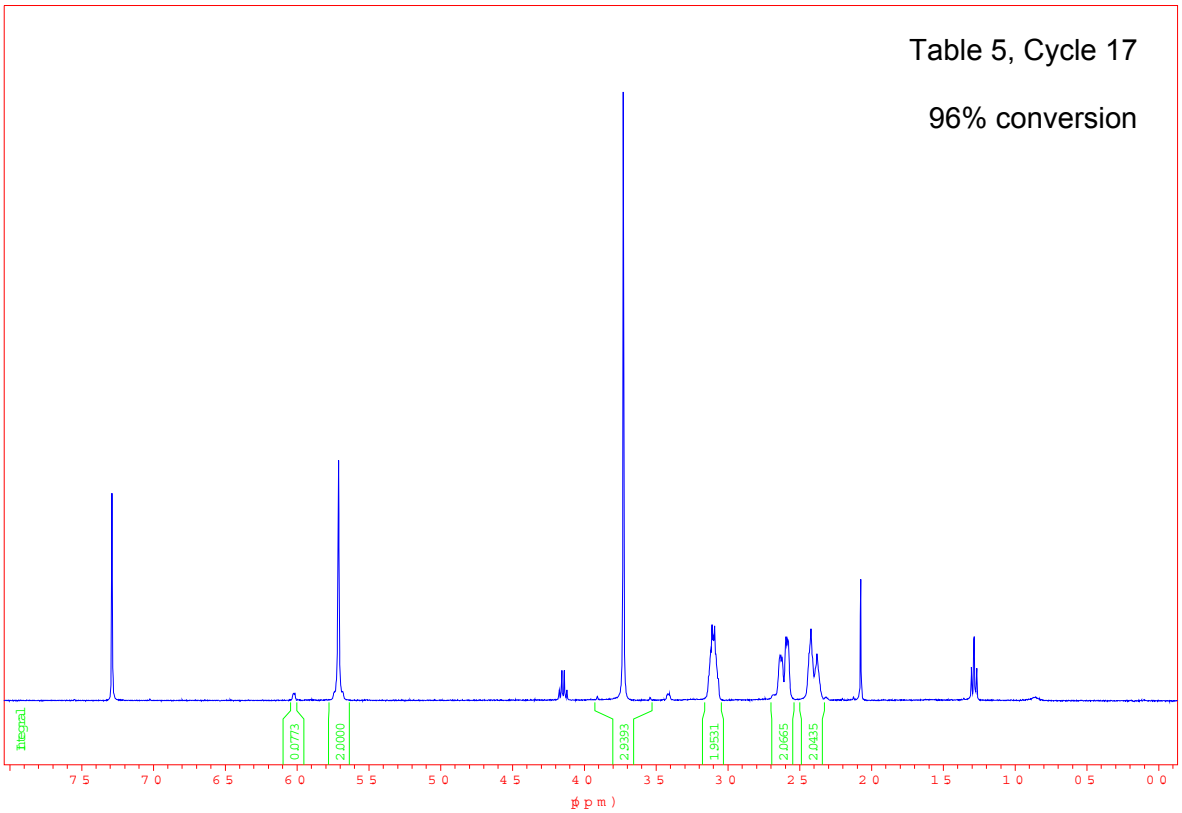

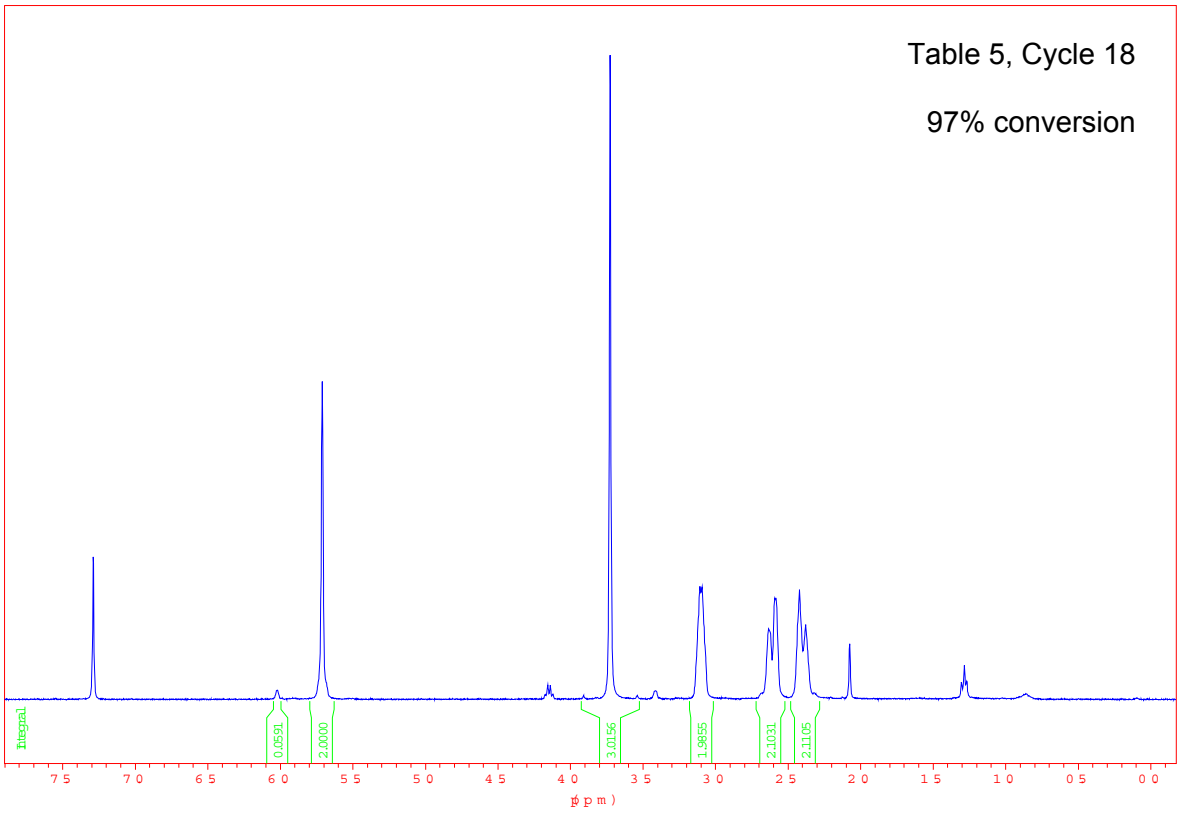

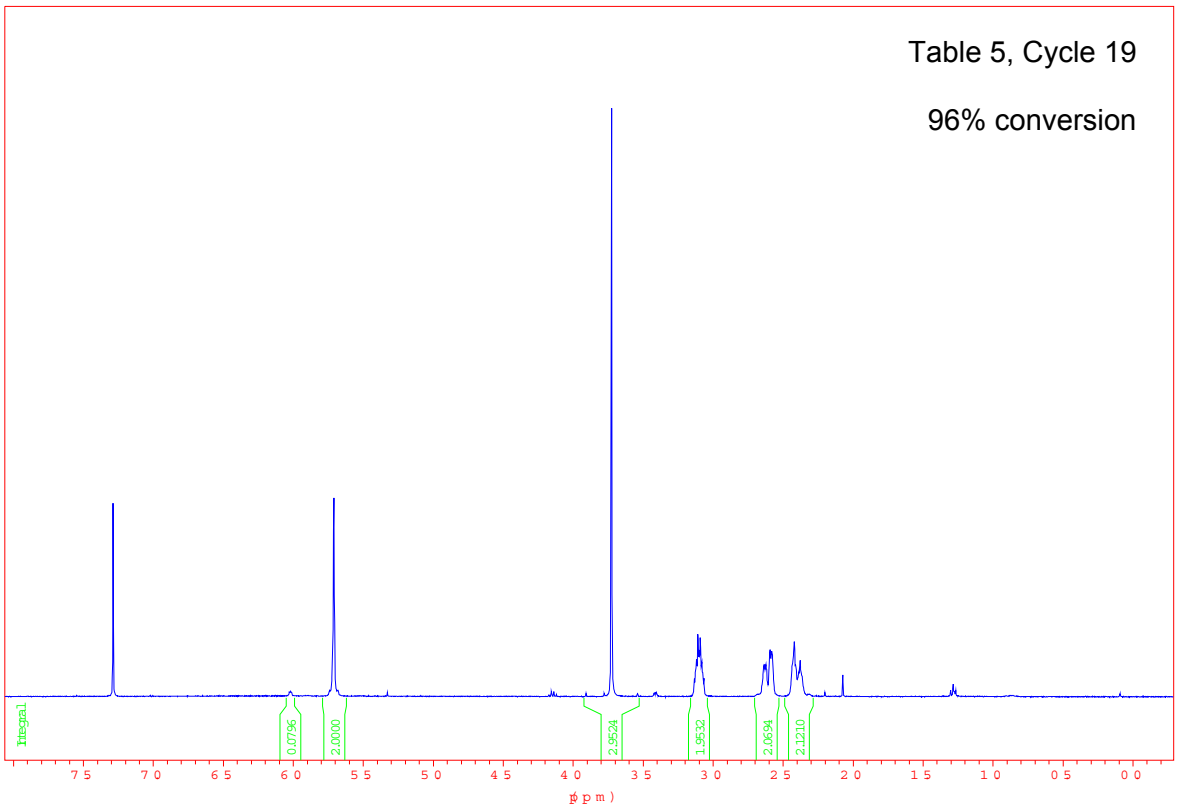

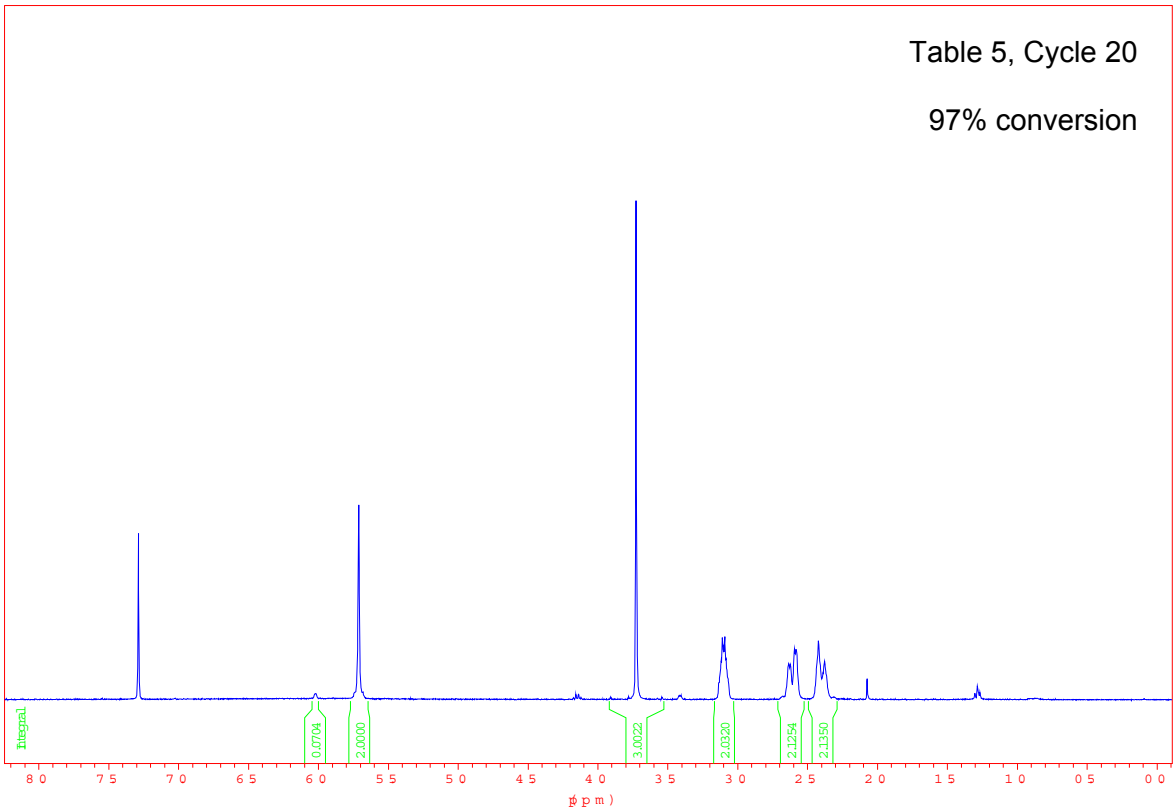

7.0 NMR spectra of hemiesters **21-23** and **28-30**

^{1}H NMR spectrum (400 MHz, $CDCl_3$) of hemiester **21**

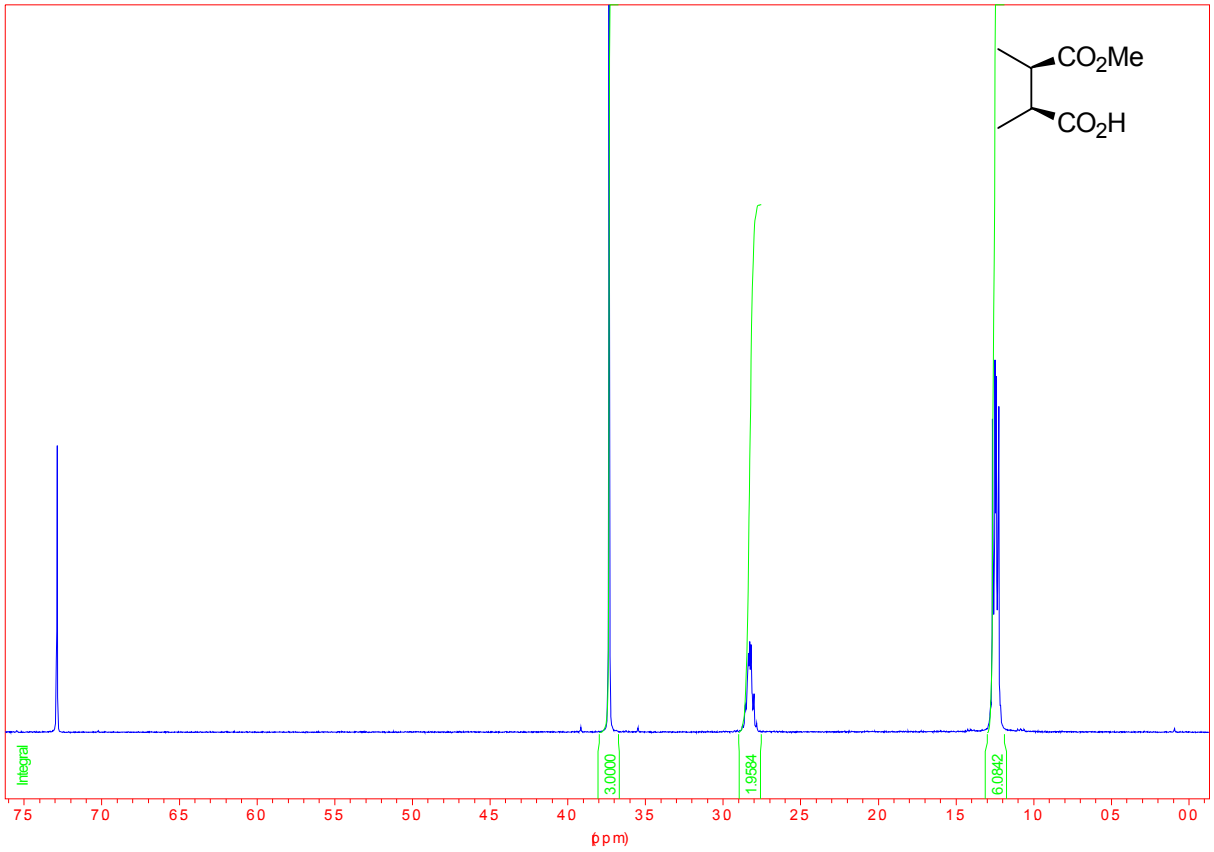

^{13}C NMR spectrum (100 MHz, $CDCl_3$) of hemiester **21**

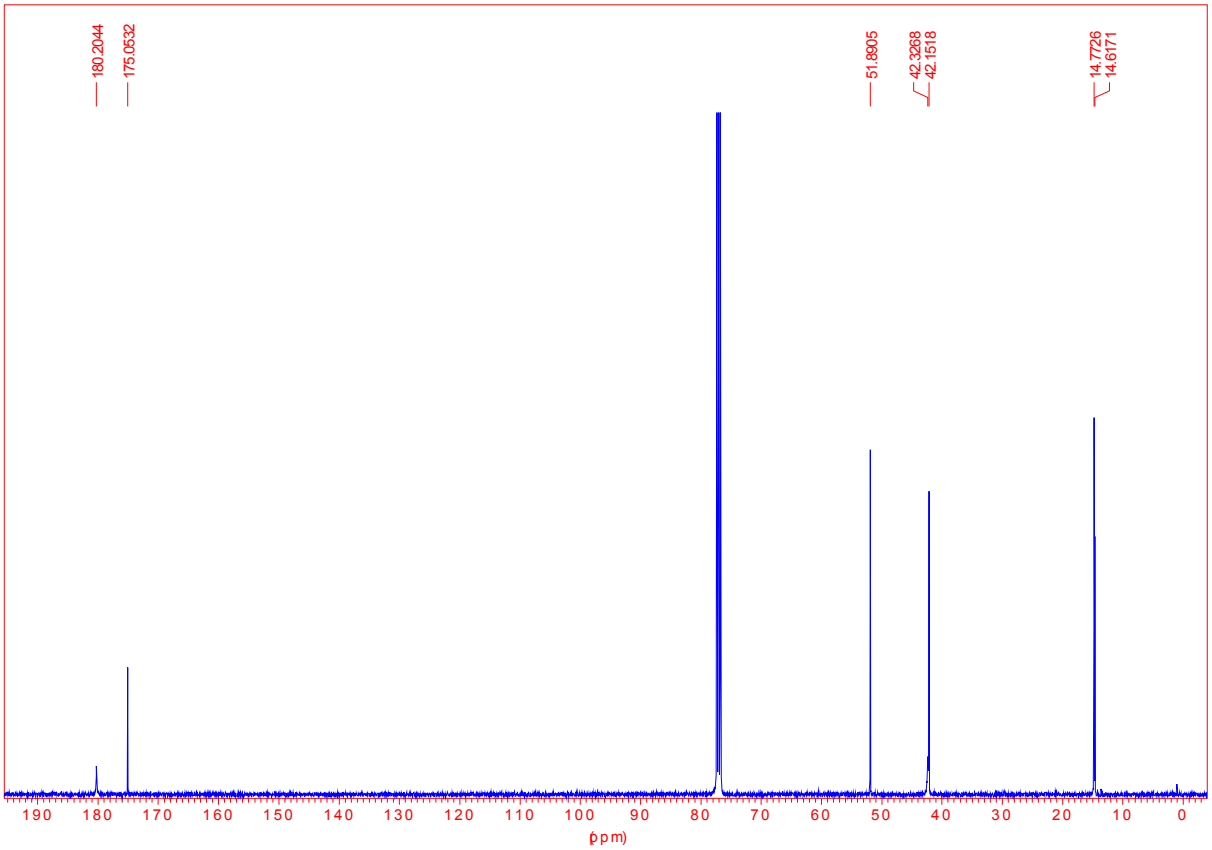

^{1}H NMR spectrum (400 MHz, $CDCl_3$) of hemiester **22**

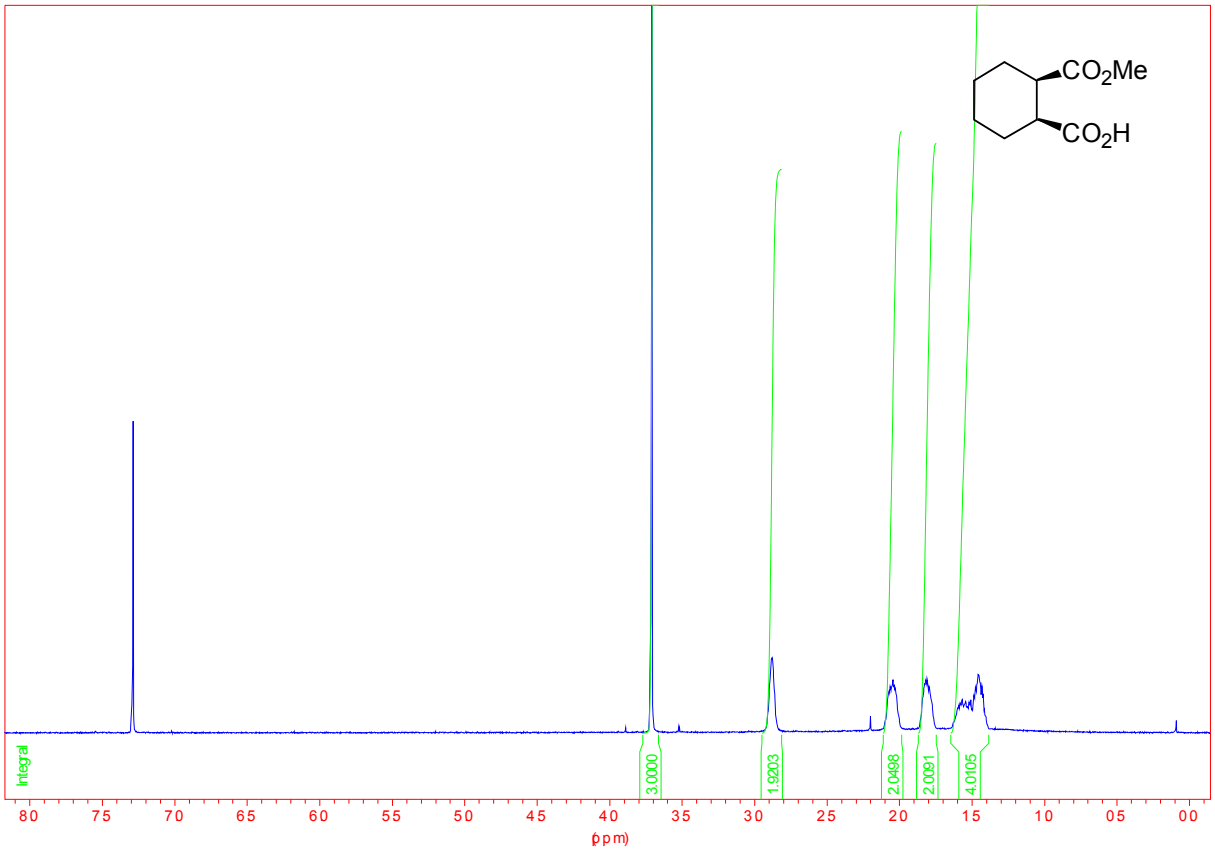

^{13}C NMR spectrum (100 MHz, $CDCl_3$) of hemiester **22**

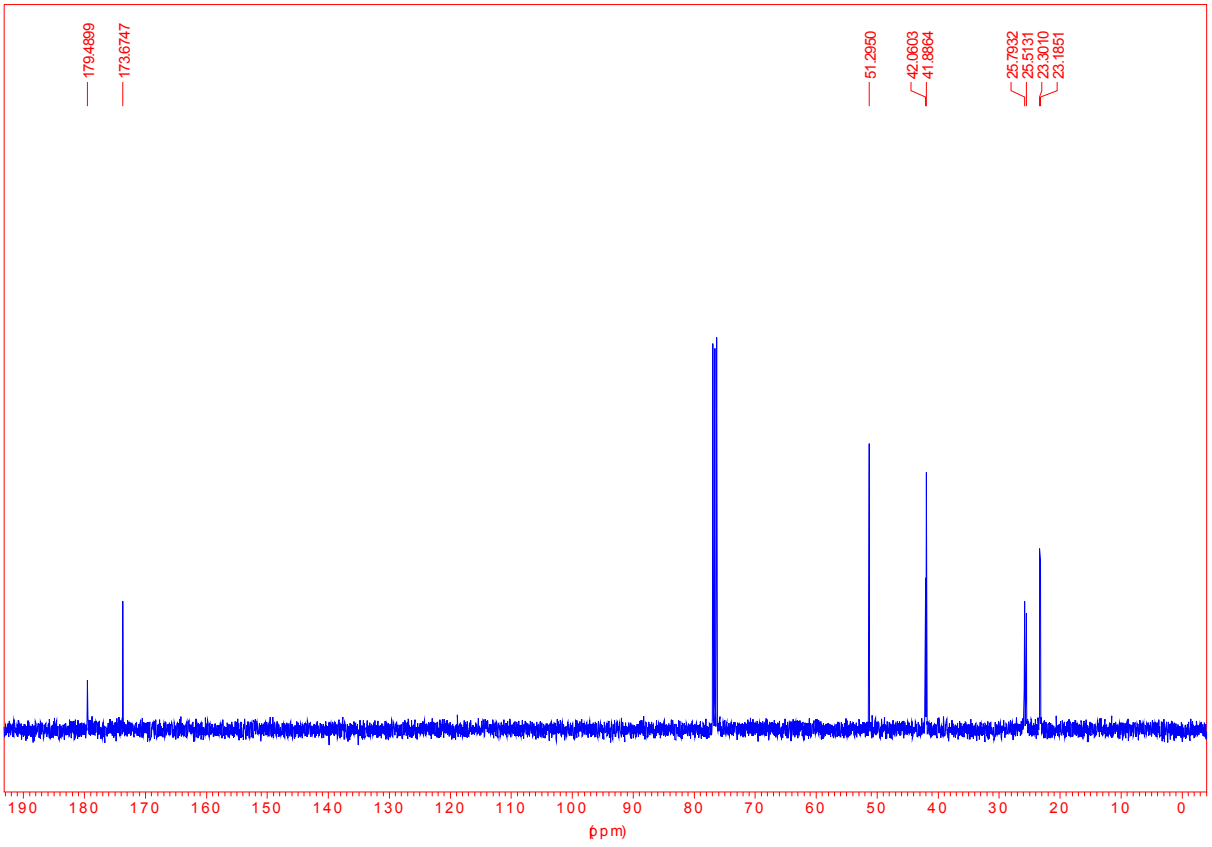

^{1}H NMR spectrum (400 MHz, $CDCl_3$) of hemiester **23**

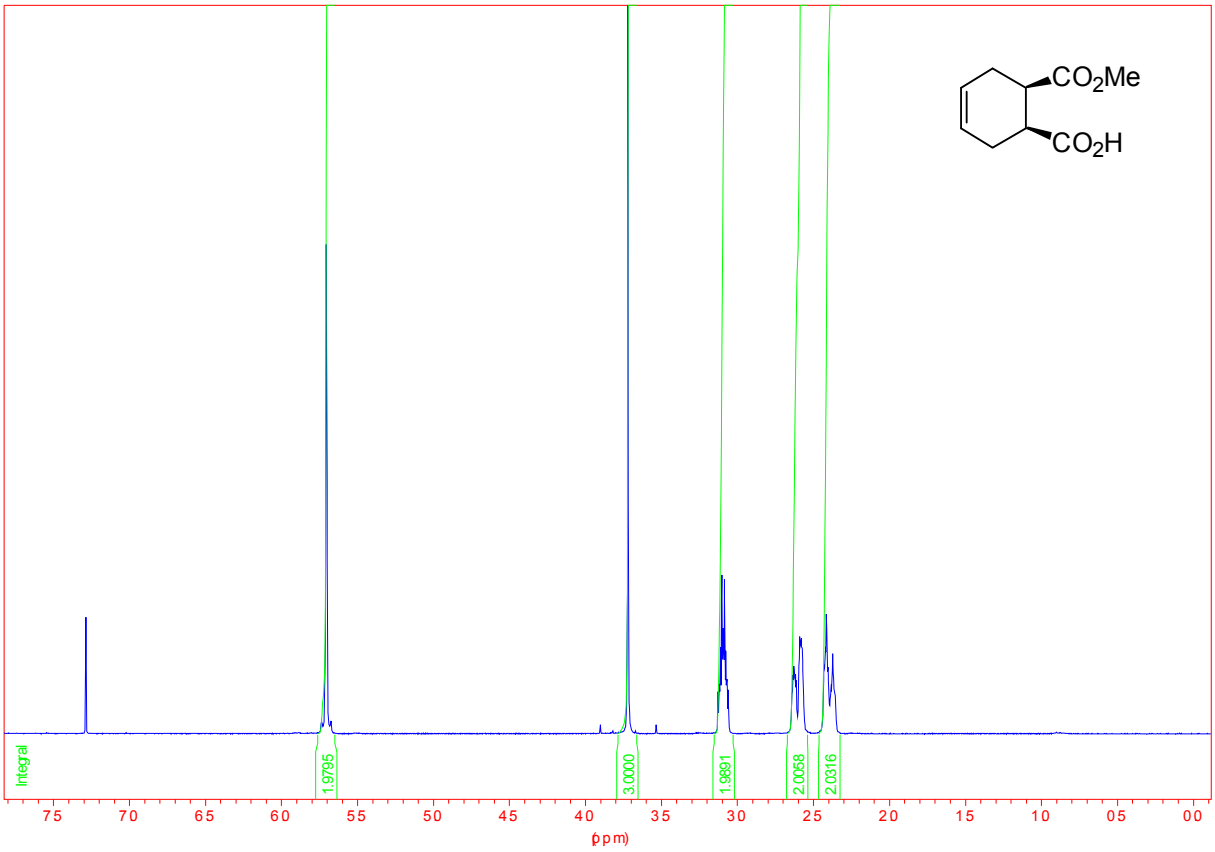

^{13}C NMR spectrum (100 MHz, $CDCl_3$) of hemiester **23**

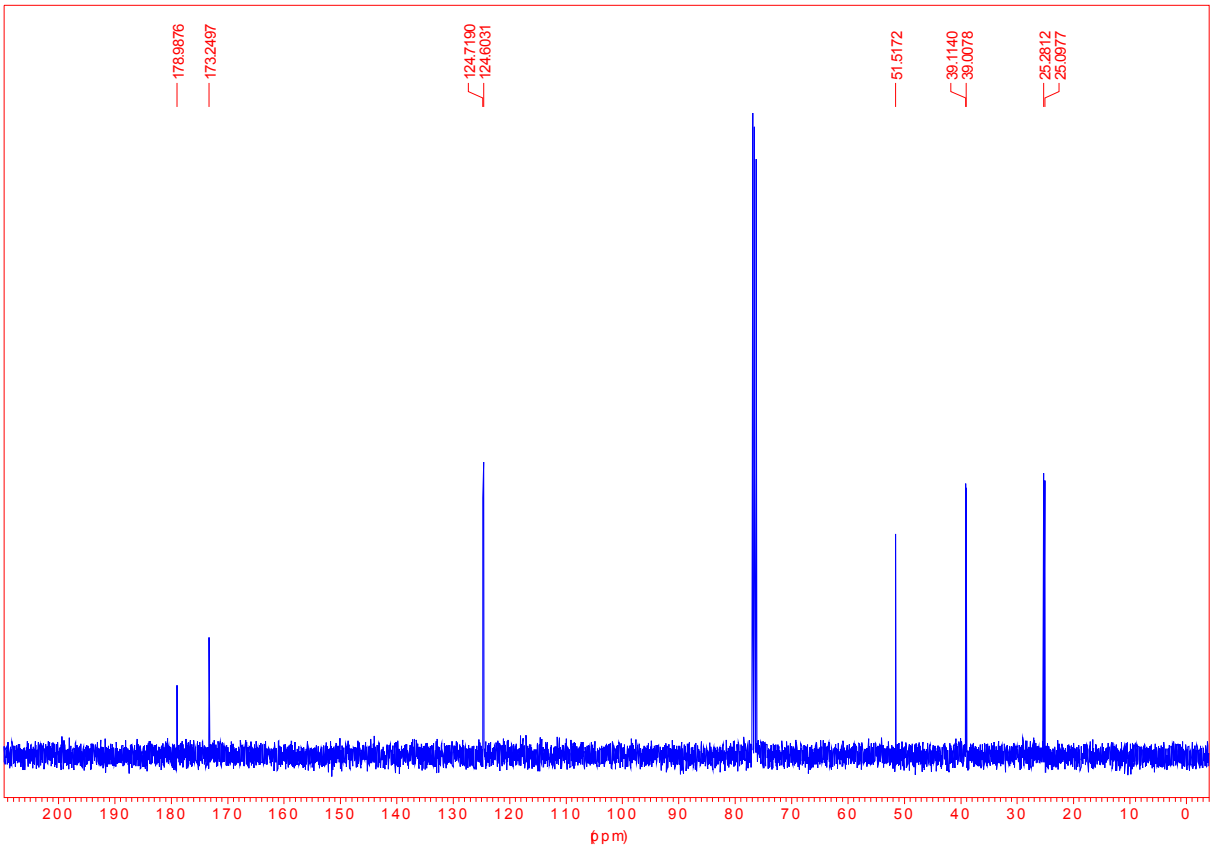

^{1}H NMR spectrum (600 MHz, $CDCl_3$) of hemiester **28**

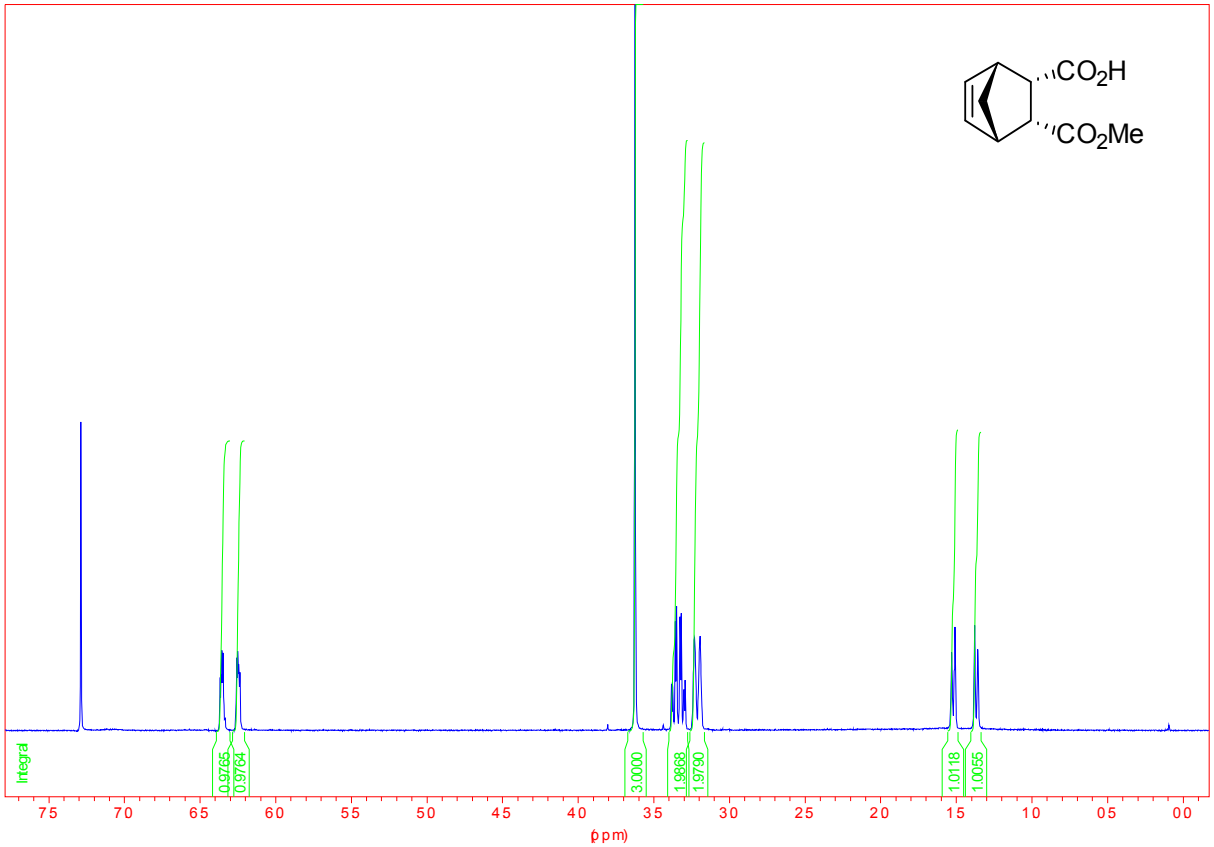

^{13}C NMR spectrum (150 MHz, $CDCl_3$) of hemiester **28**

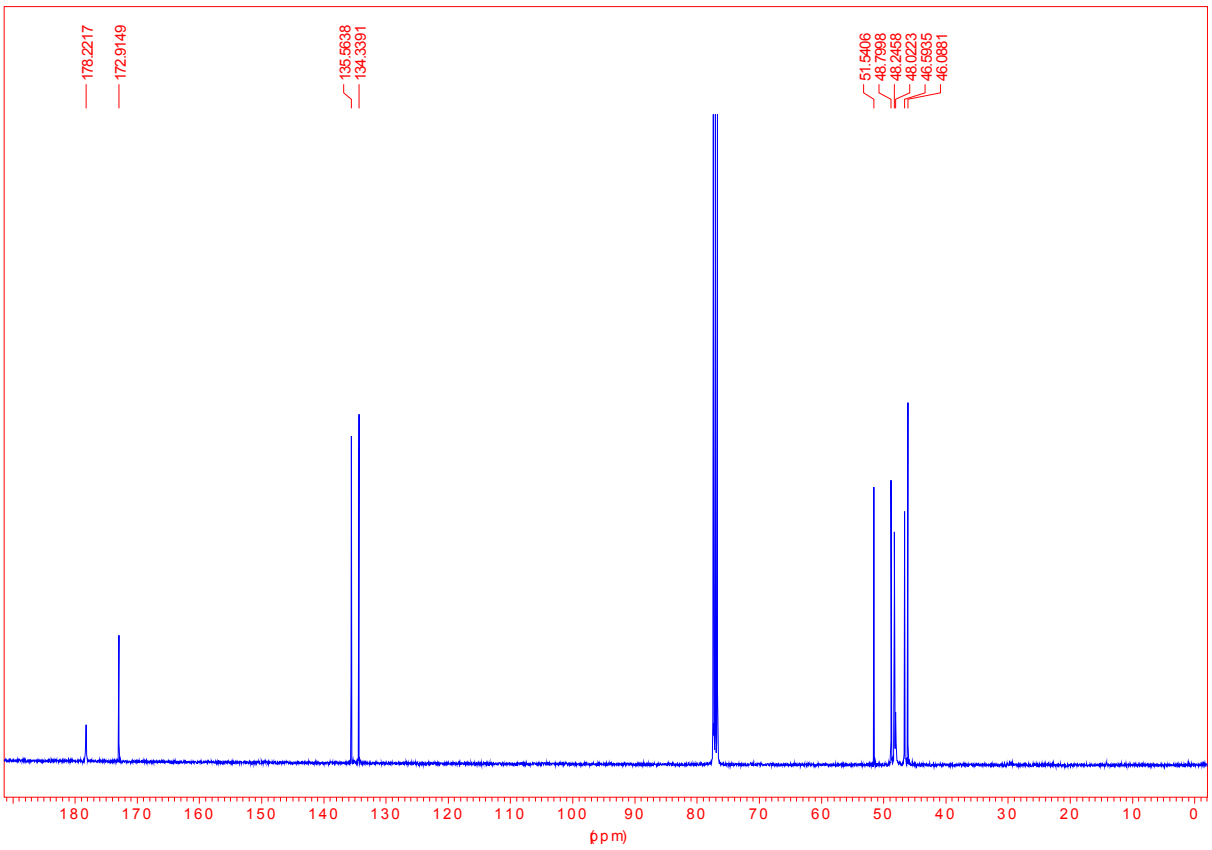

^{1}H NMR spectrum (600 MHz, $CDCl_3$) of hemiester **29**

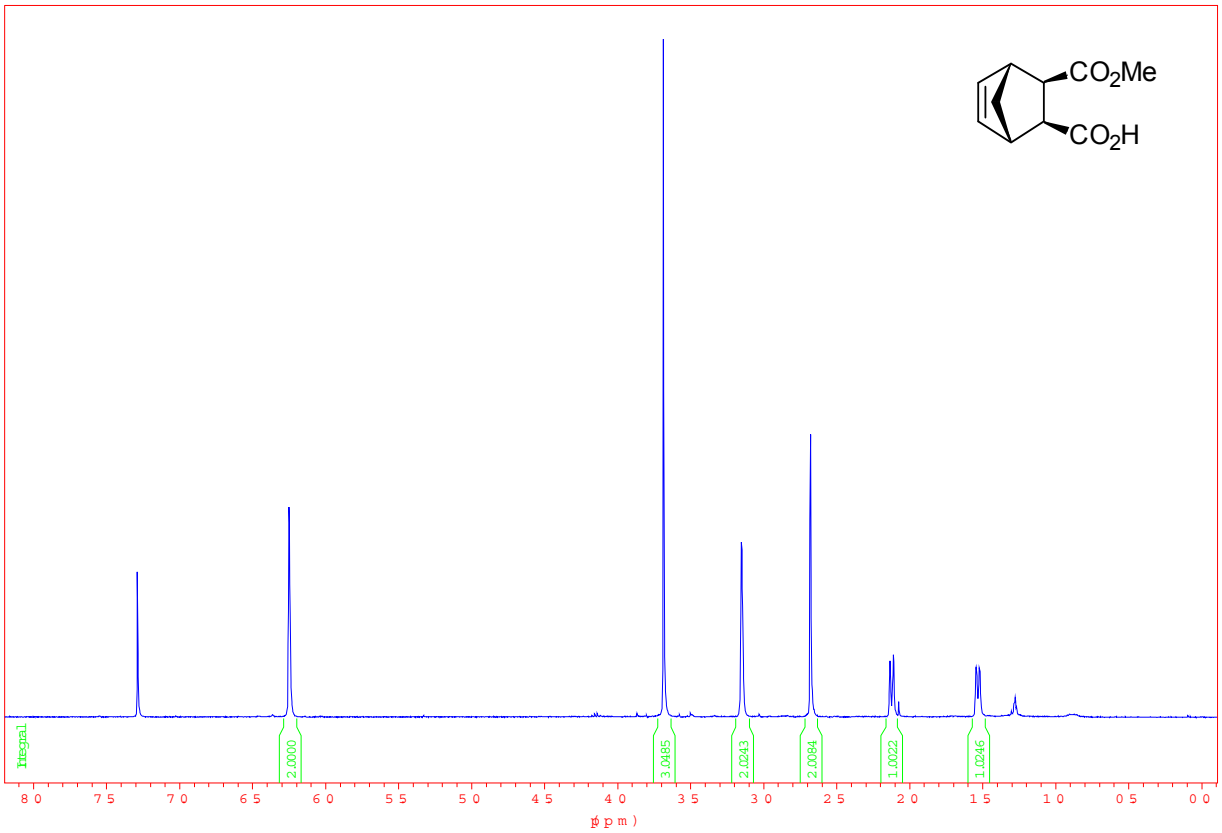

^{13}C NMR spectrum (100 MHz, $CDCl_3$) of hemiester **29**

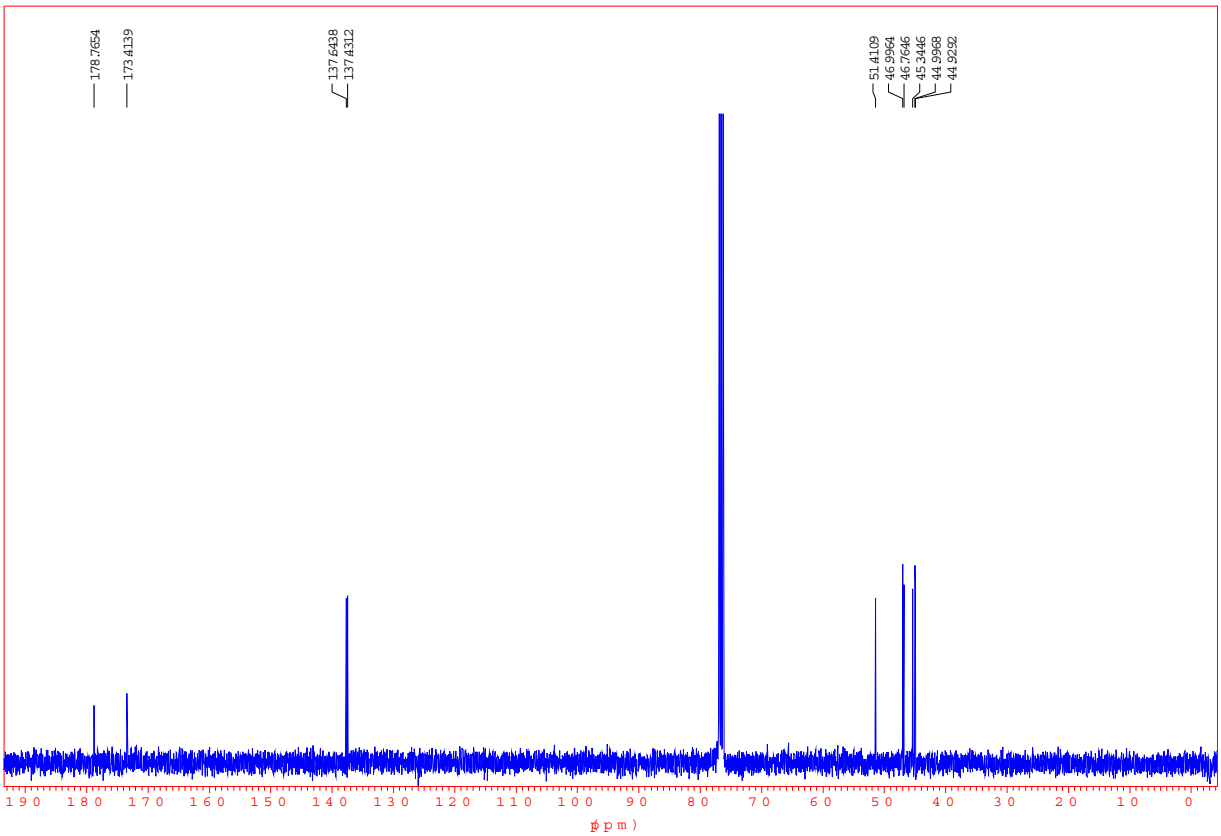

NMR spectrum (400 MHz, $CDCl_3$) of hemiester **30**

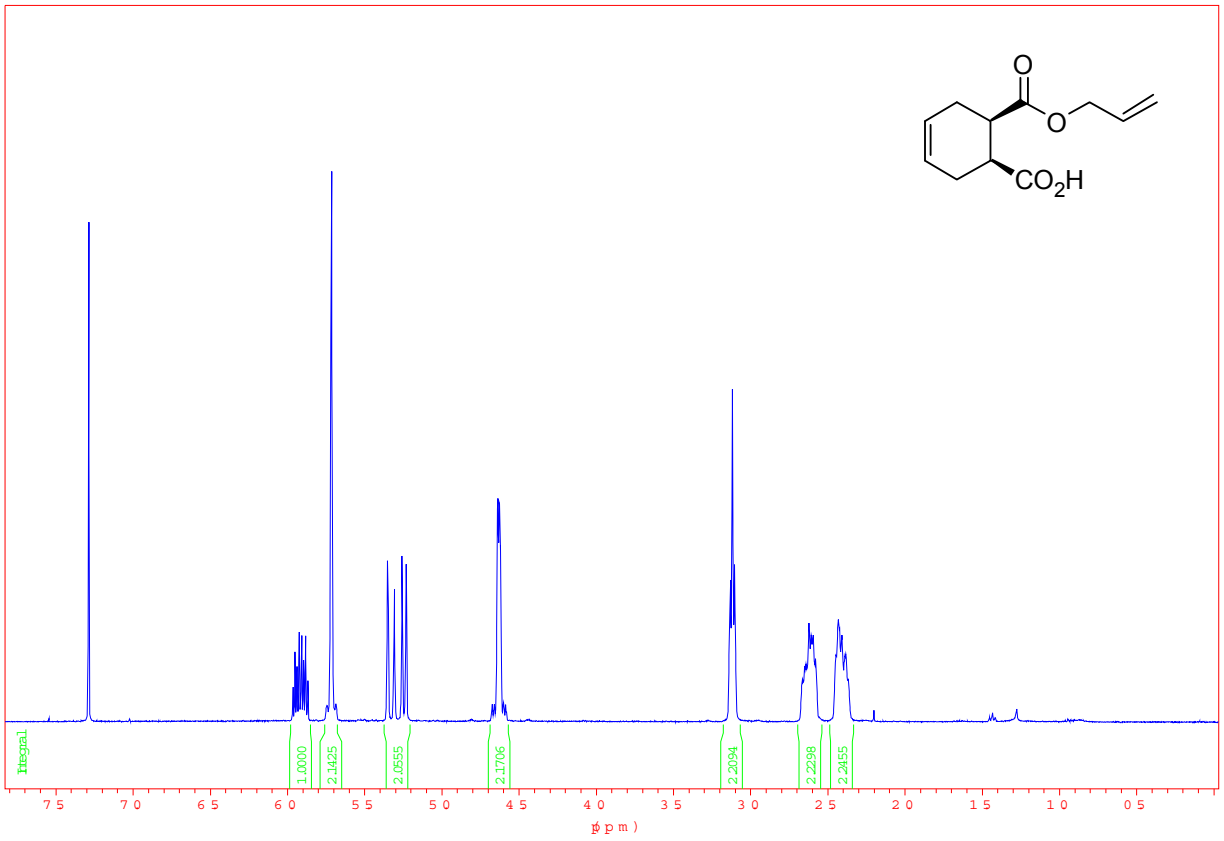

^{13}C NMR spectrum (100 MHz, $CDCl_3$) of hemiester **30**

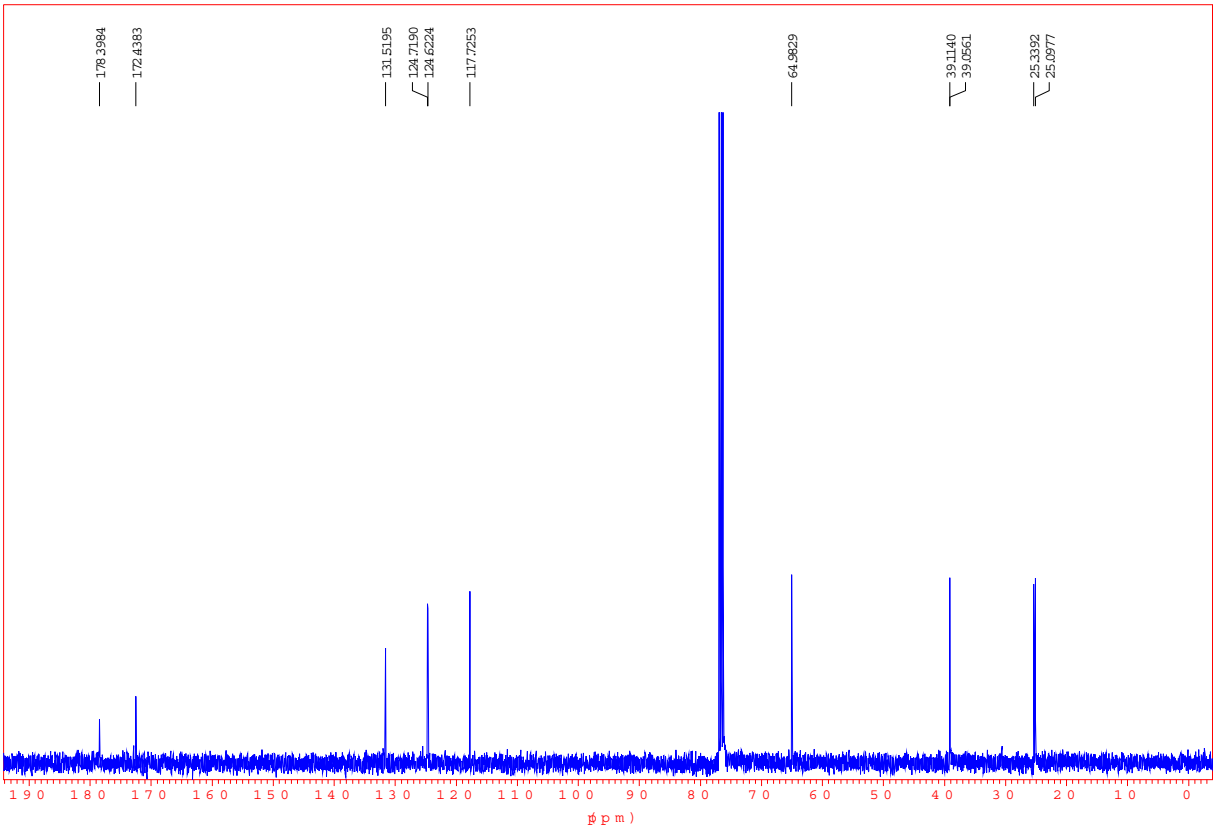

7.1 Enantiomeric excess determination of hemiesters **21-23** and **28-30** (Tables 5-6 and Schemes 4-5)

The enantiomeric excess of each hemiester product of the desymmetrisation reaction could be determined by comparison of the product methyl ester resonances in the ^{1}H NMR spectrum (and confirmed by CSP-HPLC analysis in some representative cases) after conversion of the hemiester into a diastereoisomeric mixture of amides derived from commercially available (*R*)-1-(1-naphthyl)ethylamine (Scheme 1).[2]

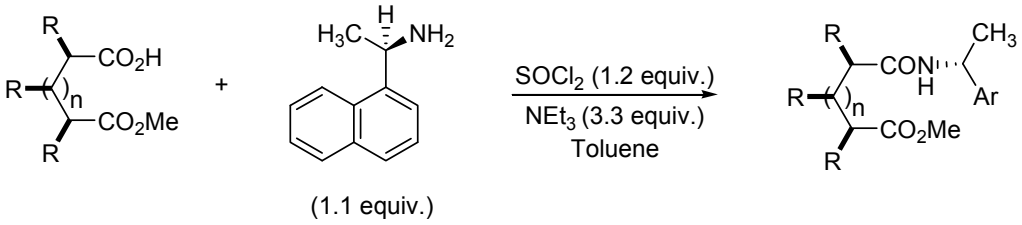

Scheme 1

Enantiomeric excess determination by ^{1}H NMR spectroscopic analysis after derivatisation

Table 5, entry 1, cycle 1, 80% *ee*

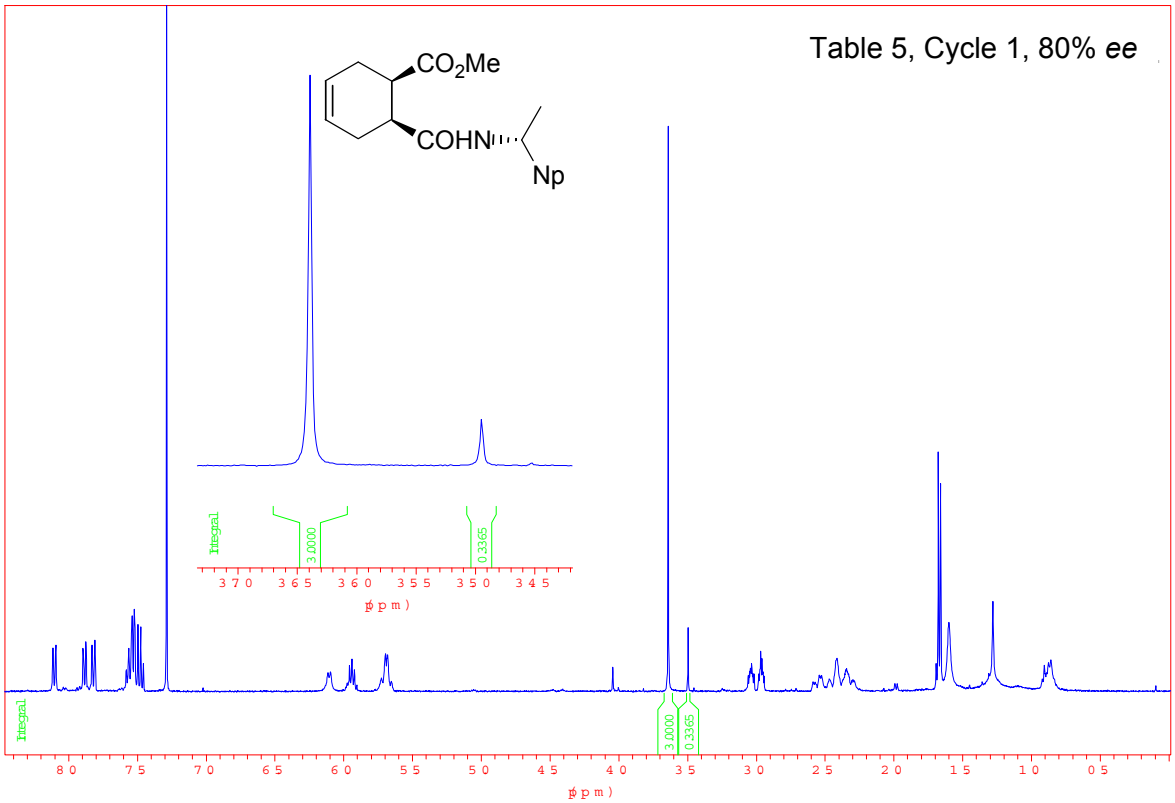

Table 5, entry 10, cycle 10, 78% *ee*

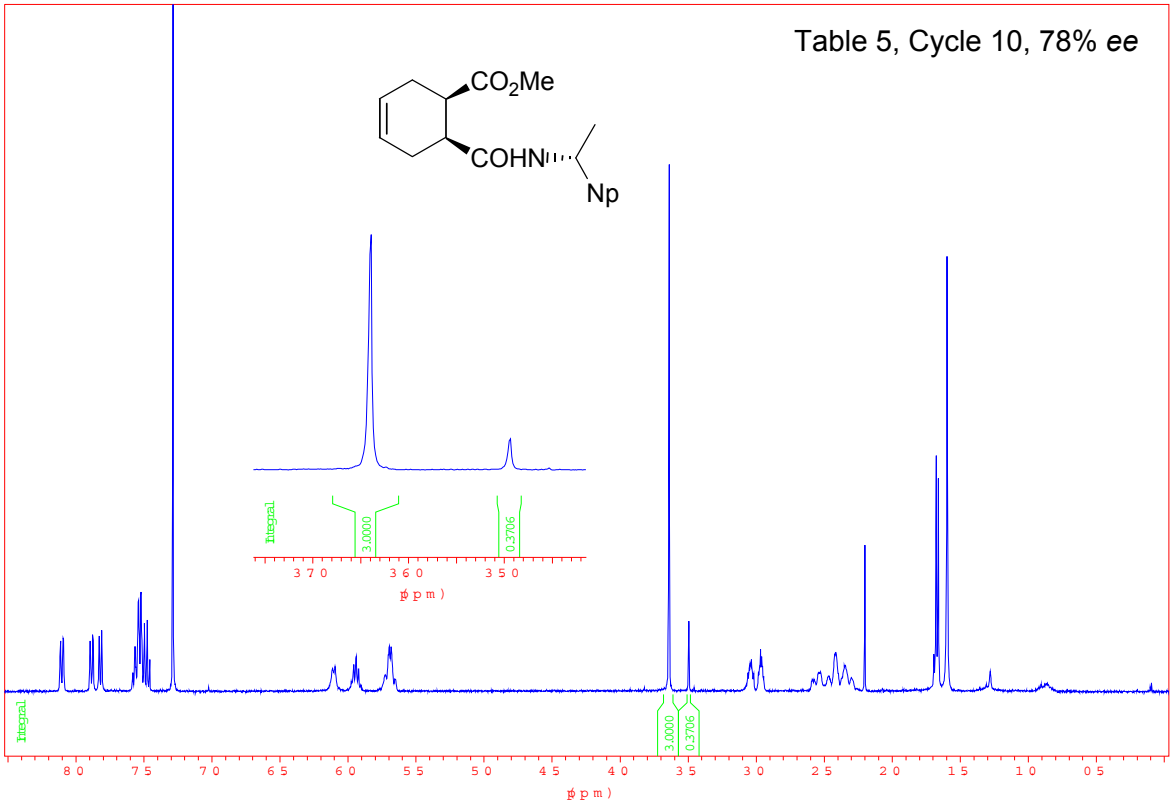

Table 5, entry 20, cycle 20, 77% *ee*

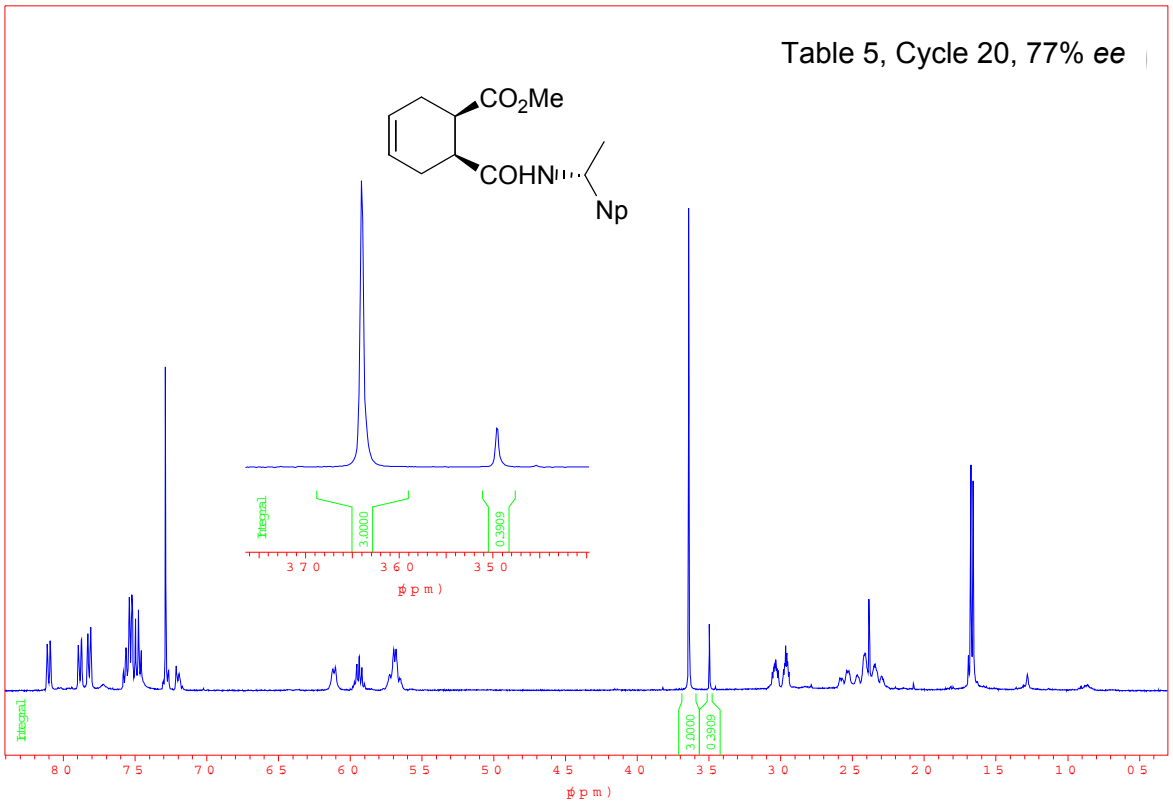

Scheme 5, cycle 30, 78% *ee*

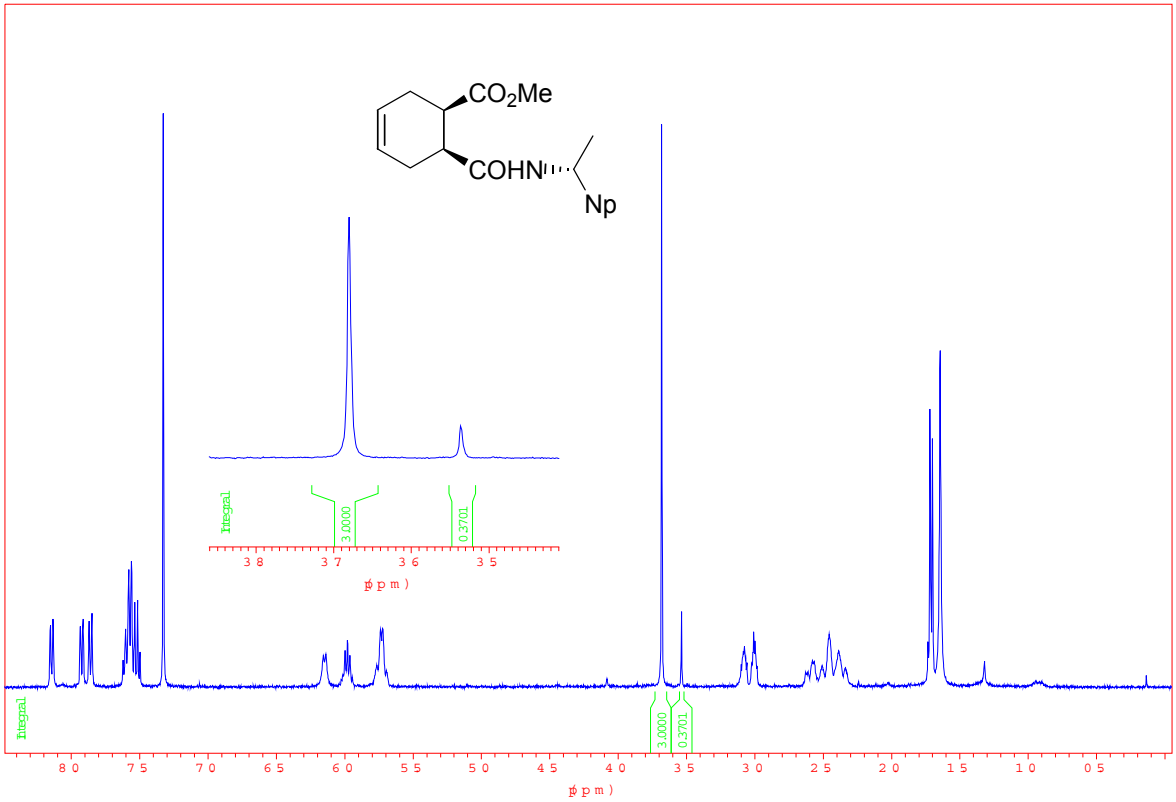

^{1}H-NMR of the diastereoisomeric mixture obtained from the racemic hemiester (400 MHz, $CDCl_3$)

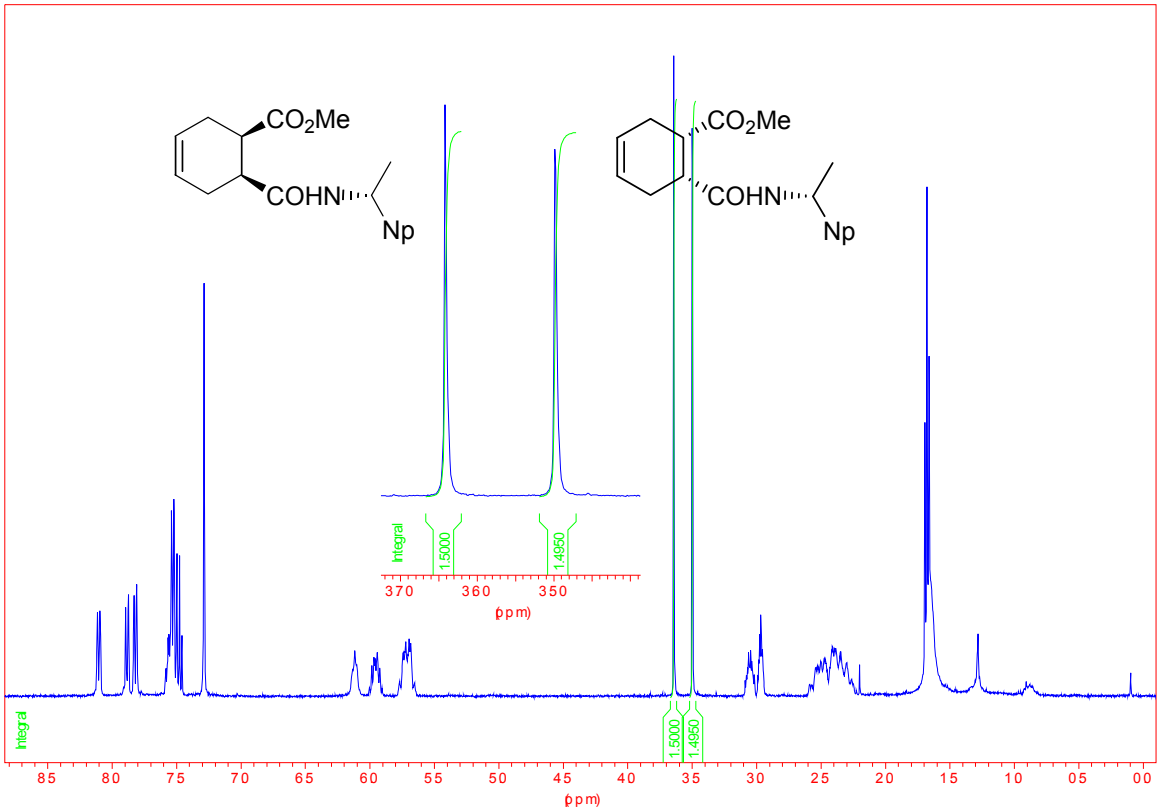

Table 6, entry 1, cycle 21, 78% *ee*

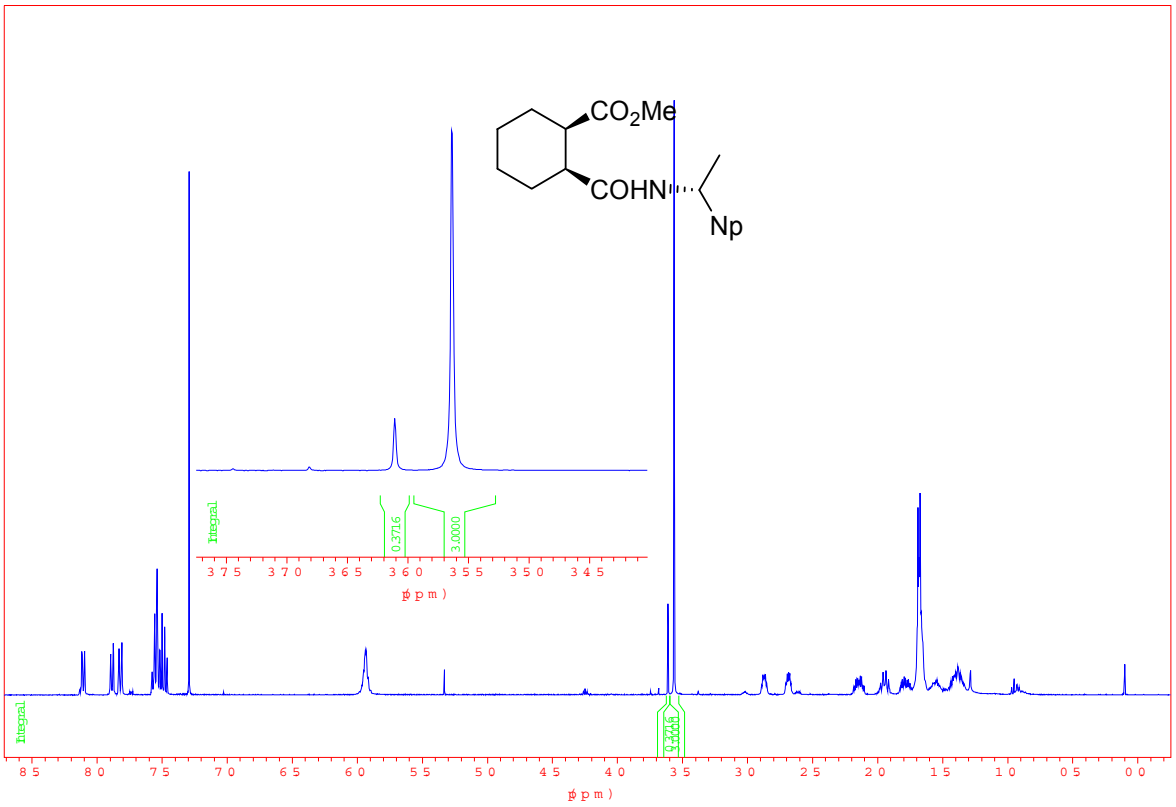

^{1}H-NMR of the diastereoisomeric mixture obtained from the racemic hemiester (400 MHz, $CDCl_3$)

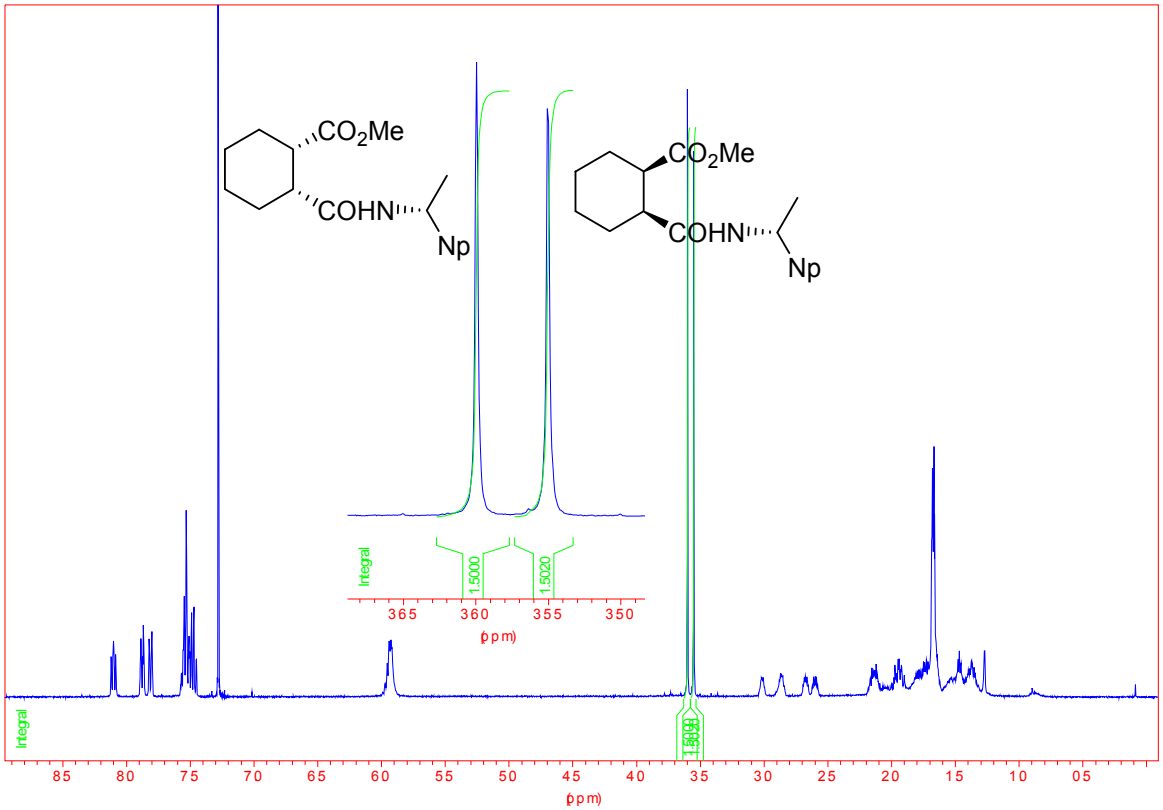

Table 6, entry 4, cycle 24, 78% *ee*

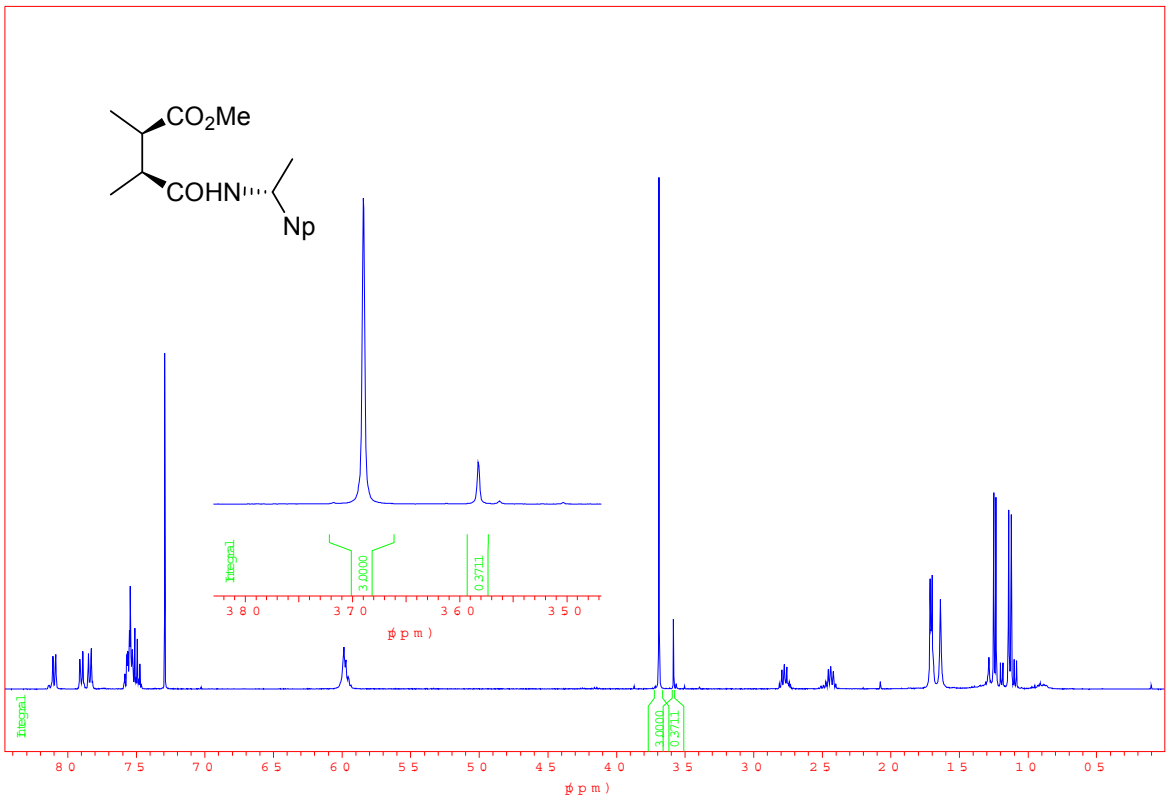

^{1}H-NMR of the diastereoisomeric mixture obtained from the racemic hemiester (400 MHz, $CDCl_3$)

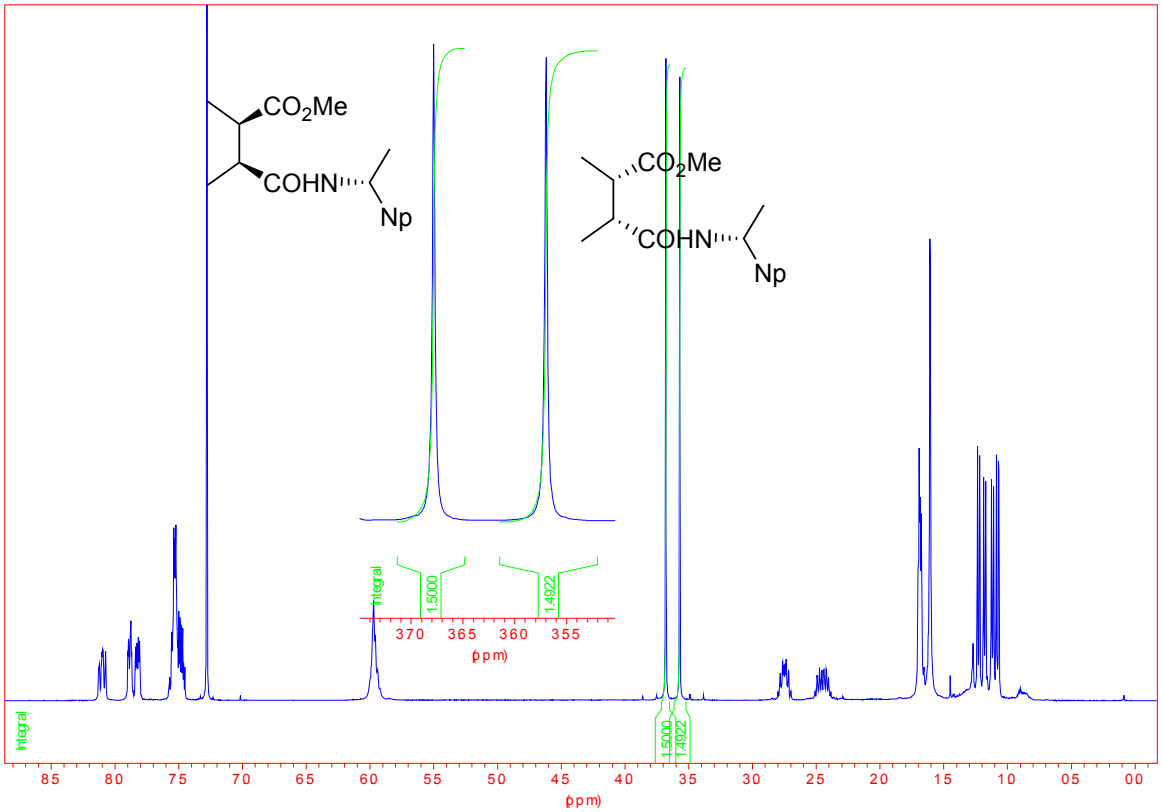

Table 6, entry 7, cycle 27, 82% *ee*

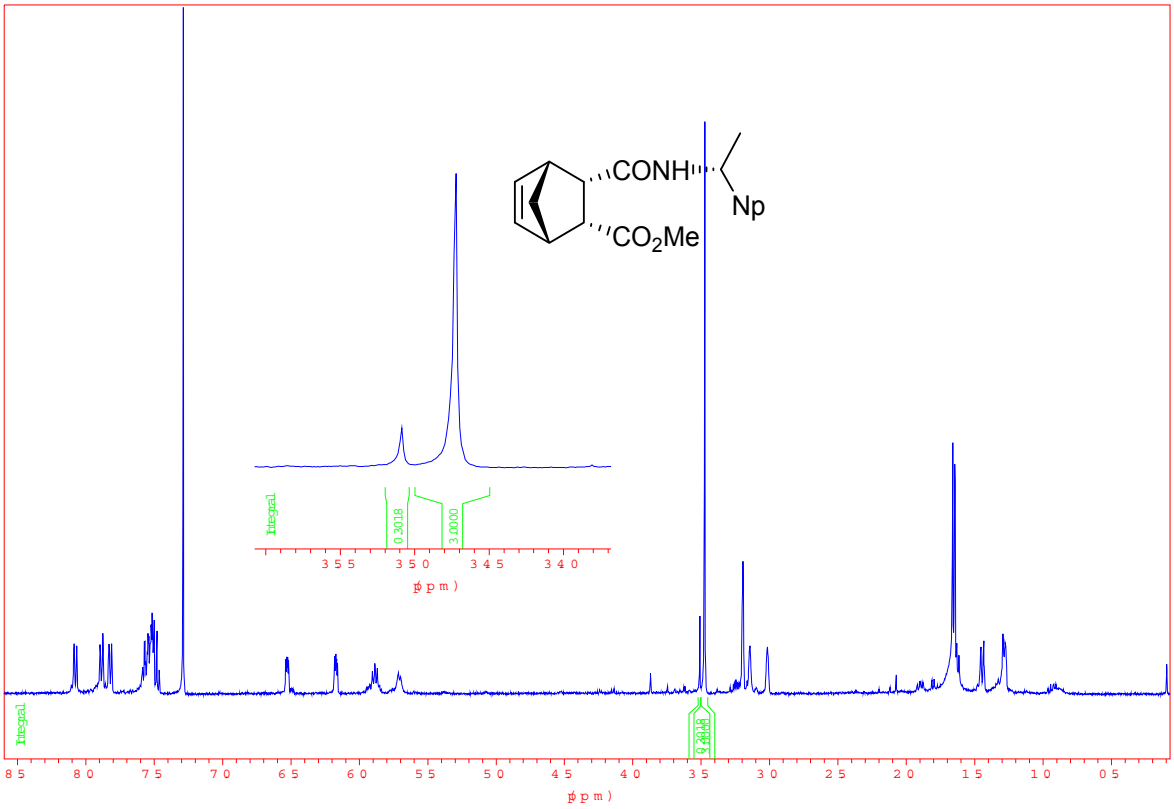

^{1}H-NMR of the diastereoisomeric mixture obtained from the racemic hemiester (400 MHz, $CDCl_3$)

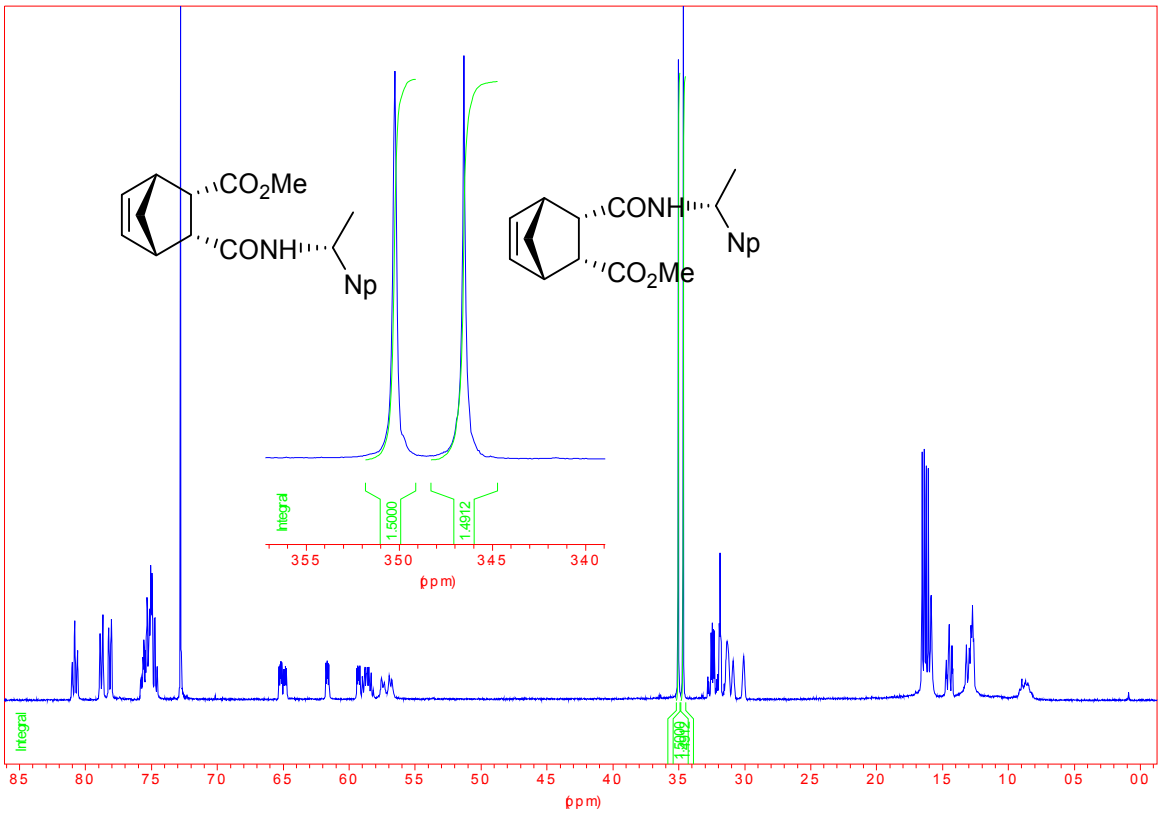

Table 6, entry 8, cycle 28, 79% *ee*

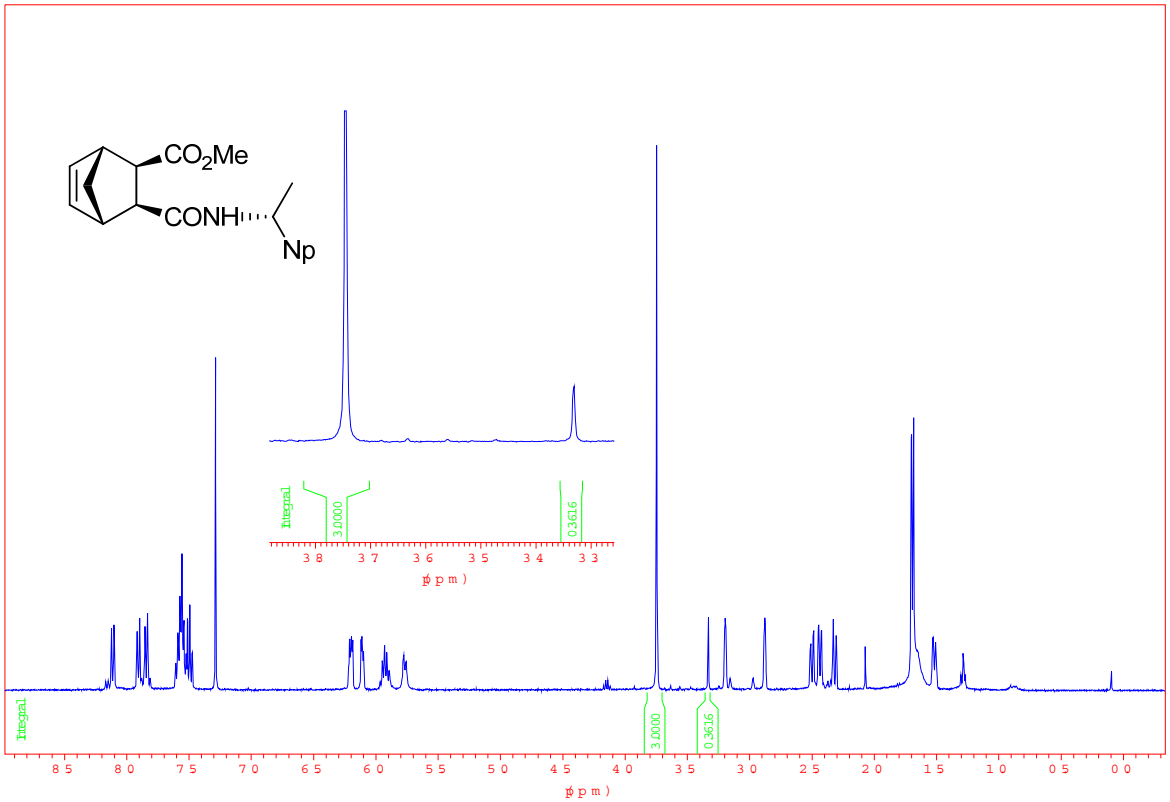

^{1}H-NMR of the diastereoisomeric mixture obtained from the racemic hemiester (400 MHz, $CDCl_3$)

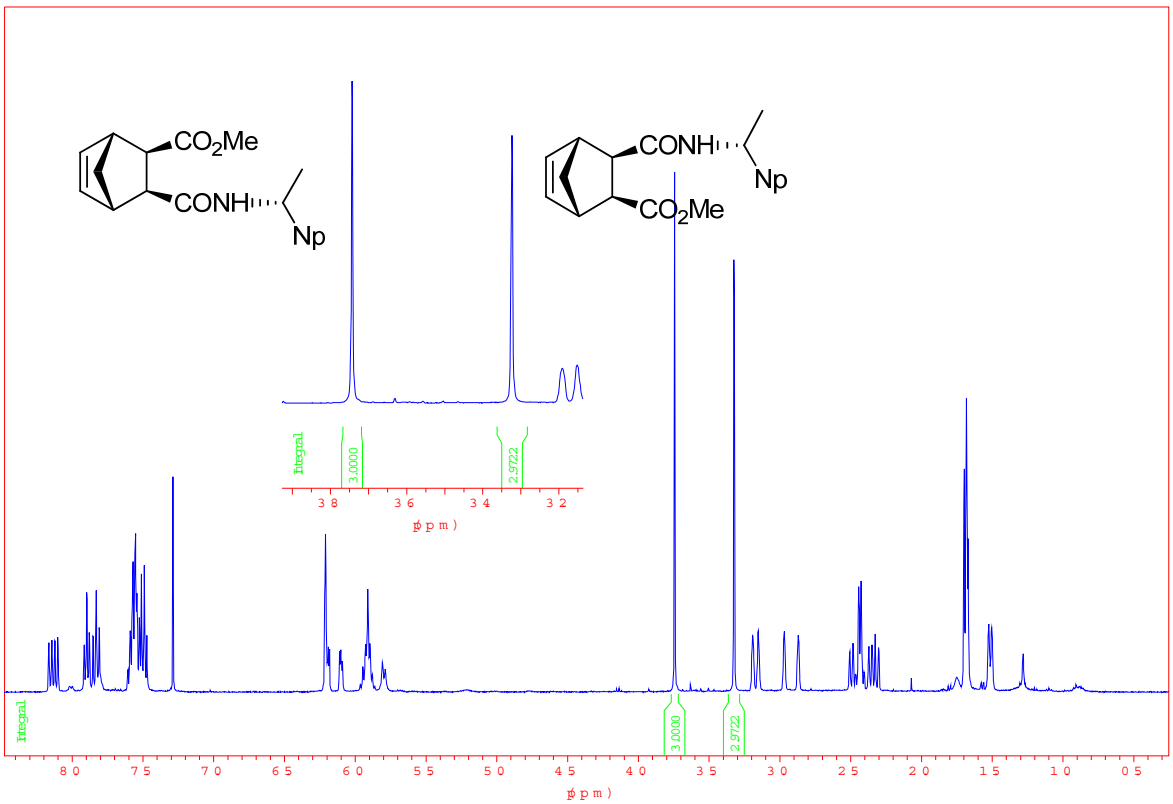

Enantiomeric excess determination by CSP-HPLC analysis after derivatisation

CSP-HPLC analysis of the diastereoisomeric mixture obtained from racemic hemiester 23

Chiralcel OD-H (4.6 mm x 25 cm), Hexane/IPA: 93/7, 0.50 mL min^{-1}, RT, UV 220 nm

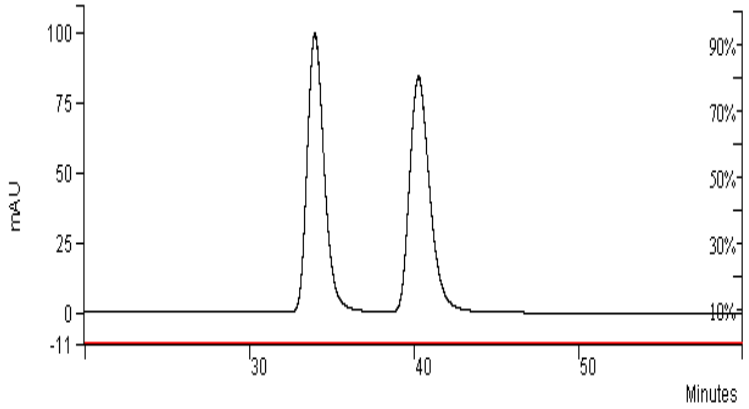

Time (min)	Result %
33.928	49.331
40.223	49.631

CSP-HPLC analysis of the diastereoisomeric mixture from enantioenriched hemiester 23

Table 5, entry 10, cycle 10, 77.5 % *ee*

Chiralcel OD-H (4.6 mm x 25 cm), Hexane/IPA: 93/7, 0.50 mL min^{-1}, RT, UV 220 nm

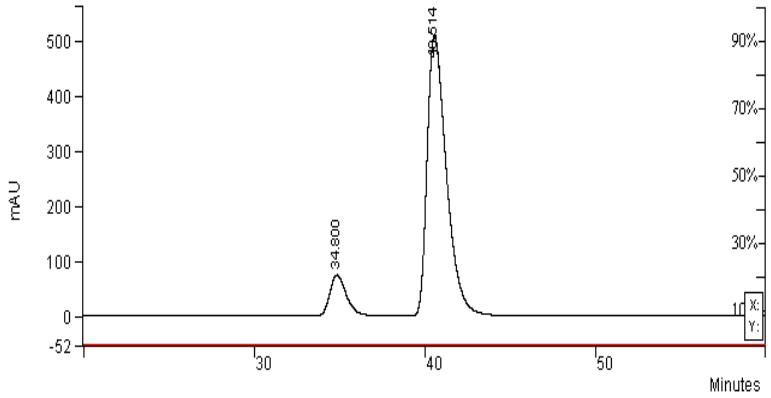

Time (min)	Result %
34.800	11.206
40.514	88.377

CSP-HPLC analysis of the diastereoisomeric mixture from racemic hemiester 30

Chiralcel OD-H (4.6 mm x 25 cm), Hexane/IPA: 95/5, 1.0 mL min^{-1}, RT, UV 220 nm

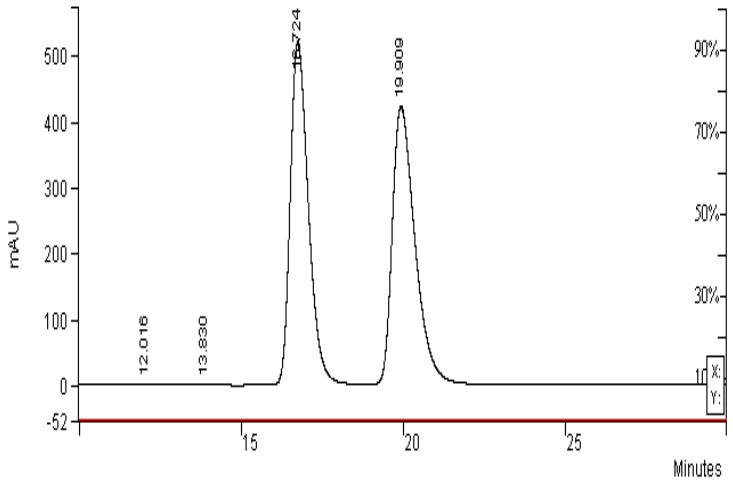

Time (min)	Result %
16.724	48.876
19.909	50.471

CSP-HPLC analysis of the diastereoisomeric mixture from enantioenriched hemiester 30

Scheme 4, cylce 29, 82% *ee*

Chiralcel OD-H (4.6 mm x 25 cm), Hexane/IPA: 95/5, 1.0 mL min^{-1}, RT, UV 220 nm

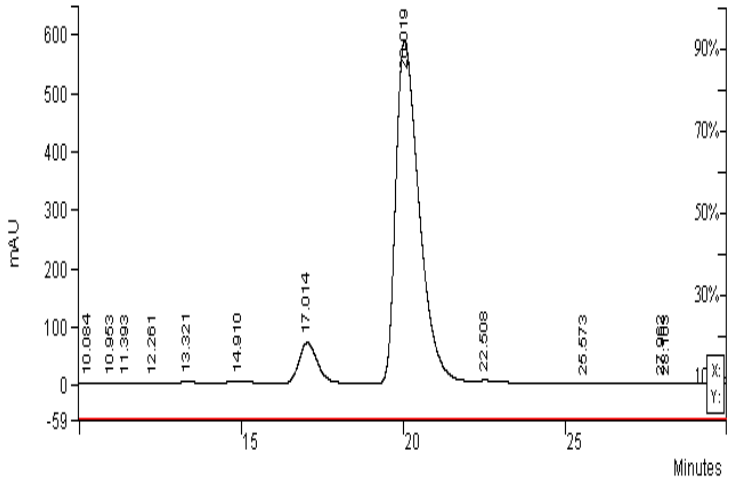

Time (min)	Result %
17.014	8.703
20.019	88.222

References

1 R.M. Cornell, U. Schwertmann, The Iron Oxides, Wiley VCH Verlag GmbH and Co., Weinheim, **1996**.

2 J. Hiratake, M. Inagaki, Y. Yamamoto and J. Oda, *J. Chem. Soc. Perkin Trans. I,* 1987, 1053.